ISSN 0252-1075
Contribution from IITM
Research Report No. RR-140
ESSO/IITM/PDTC/SR/02(2018)/191

The vertical wind tunnel facility at IITM - A review of laboratory experiments on cloud microphysics

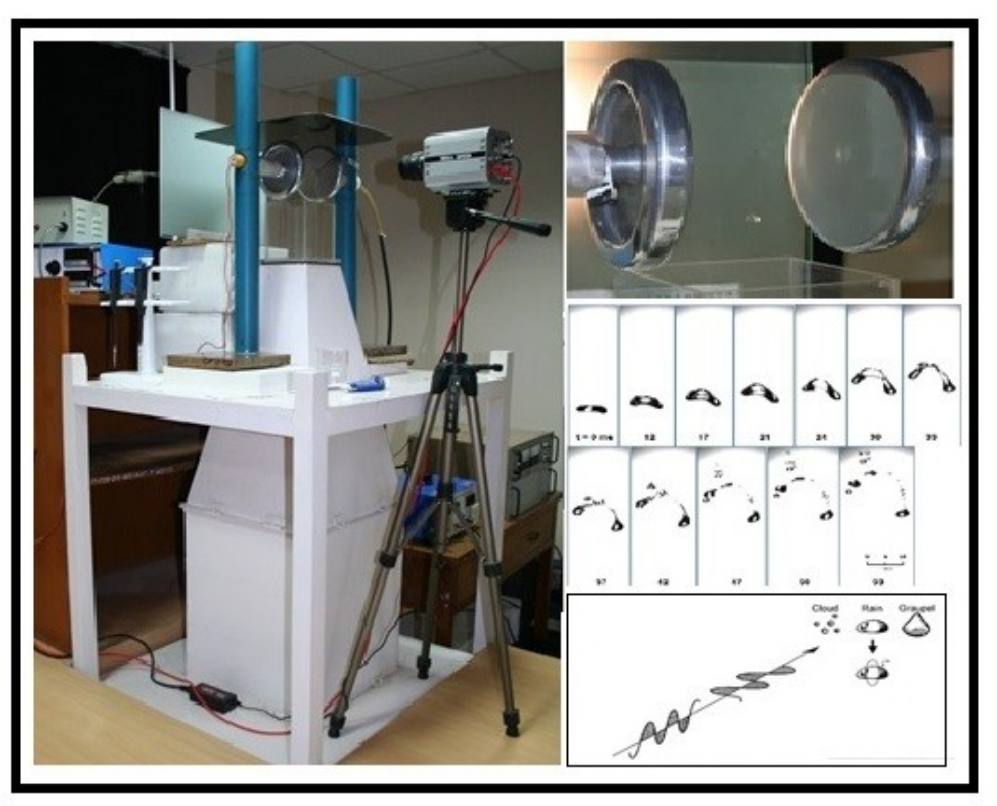

A.K. Kamra, Rohini Bhalwankar and C.G. Deshpande

Indian Institute of Tropical Meteorology (IITM)
Earth System Science Organization (ESSO)
Ministry of Earth Sciences (MoES)
PUNE, INDIA
http://www.tropmet.res.in/

ISSN 0252-1075
Contribution from IITM
Research Report No. RR-140
ESSO/IITM/PDTC/SR/02(2018)/191

The vertical wind tunnel facility at IITM - A review of laboratory experiments on cloud microphysics

A.K. Kamra, Rohini Bhalwankar and C.G. Deshpande

***Corresponding Author Address:**
Mrs. Rohini Bhalwankar
Indian Institute of Tropical Meteorology,
Dr. Homi Bhabha Road, Pashan, Pune – 411 008, INDIA
E-mail: rohini@tropmet.res.in
Phone: +91-20-25904286

Indian Institute of Tropical Meteorology (IITM)
Earth System Science Organization (ESSO)
Ministry of Earth Sciences (MoES)
PUNE, INDIA
http://www.tropmet.res.in/

DOCUMENT CONTROL SHEET

Earth System Science Organization (ESSO)
Ministry of Earth Sciences (MoES)
Indian Institute of Tropical Meteorology (IITM)

ESSO Document Number
ESSO/IITM/PDTC/SR/02(2018)/191

Title of the Report
The vertical wind tunnel facility at IITM - A review of laboratory experiments on cloud microphysics

Authors
A.K. Kamra, Rohini Bhalwankar and C.G. Deshpande

Type of Document
Scientific Report (Research Report)

Number of pages and figures
64, 24

Number of references
131

Keywords
Wind tunnel experiments, Raindrop shape, Raindrop breakup, Drop-size distribution, Polluted thunderclouds, Corona from raindrops, Lightning enhancement

Security classification
Open

Distribution
Unrestricted

Date of Publication
March 2018

Abstract
The aim of this report is to document and summarize the results obtained in our wind tunnel experiments for a variety of phenomenon which need to be accounted in our understanding of the interactions of cloud electrification with its microphysics. The vertical wind tunnel developed at IITM has proved to be a good facility to investigate several critical problems in cloud microphysics. Several experiments conducted over last more than three decades in this wind tunnel provided some novel observations and large photographic data captured using a High Speed Camera on the deformation, oscillation, evaporation and breakup characteristics of charged/uncharged water drops of different sizes in absence/ presence of electric fields. However, in order to fill up the gap between the past studies

mostly conducted under vertical configuration of electric field, main focus in our experiments was to study the effect of horizontal electric field (E_H) on various microphysical processes in thunderclouds. This work has been extended by performing experiments on breakup of polluted and unpolluted water drops in electric field. The data has revealed some novel features of various microphysical processes occurring inside the thunderclouds.

Summary

Laboratory simulation experiments play an important role in studying the cloud and rain processes under controlled conditions. Results of our wind tunnel experiments convincingly show that the electrical forces progressively enhance the horizontal elongation of the drop but do not show any significant change in their oscillation frequency in the horizontal electric field E_H of upto 500 kVm^{-1}. The influence of strong E_H on different stages of deformation and eventual breakup of water drops has been observed using high-speed photography. In conformity with the past studies, the dumbbell, filament and bag modes of drop breakup have been observed when E_H=0. However, drops elongate in horizontal direction, mostly develop sharp curvature at their ends, eject a fine jet spray of tiny droplets and ultimately break up into several charged / uncharged droplets when E_H=500 kVm^{-1}. A 7.0 mm diameter drop has been observed to undergo extreme elongation of upto 29mm. Moreover, our observations of corona occurring at the surface of distorted raindrops freely suspended in our wind tunnel in E_H may explain triggering of a lightning discharge in highly electrified regions of thundercloud.

Our results also demonstrate that the enhanced distortion of the water drops falling in E_H when the drops are polluted with sulfate/nitrate salts. The difference in electrical conductivity of polluted and unpolluted water drops is most likely the key factor for manifestation of these differences. It is proposed that the enhanced distortion of polluted drops coupled with the change in their characteristics to trigger and propagate a discharge in lower electric fields may significantly contribute to explain the enhancement of lightning activity generally observed in the clouds formed over big cities.

Our experiments convincingly demonstrate that the electrical forces can strongly influence and modify the size and charge distribution of drops prevailing in different regions of a thundercloud. Consequently, the development of rain by collision-coalescence process is influenced by electrical forces. This change in size distribution of cloud drops may modify the radar echo–precipitation relationships in regions of thunderclouds with different directions of electric field. Therefore, the effect of electrical forces on microphysical characteristics needs to be accounted for better understanding of the in-cloud processes and rainfall estimation in radar meteorology.

Contents

1. Introduction

Clouds play an important role in the climate system of the Earth. Manifestation of several dynamical, microphysical and electrical processes and their mutual interactions in the clouds result in occurrence of the rainfall, the most desired component of global water cycles along with the spectacular phenomenon of the lightning. In warm clouds, raindrops are formed by "Chain reaction'' involving several microphysical processes such as the nucleation, condensation, collision, coalescence, breakup, and evaporation of drops [Langmuir, 1948]. These processes contribute to the evolution of raindrop size distribution (DSD) and are important in determining the development of rain in warm clouds. Raindrops in clouds are electrically charged and quite often are located in intense electric field regions of thunderstorms. The aim of the current report is to document a comprehensive framework for various interactions that take place between cloud microphysical processes and electrification. Knowledge of such interactions is essentially required to be considered to find out the relevant parameterizations for phenomena such as modification of the collision–coalescence efficiencies, distortion, disruption, fall velocity and evaporation of the raindrops and lightning initiation in thunderclouds. The key parameters in studying these microphysical processes are the shape and oscillations of a raindrop falling in air at its terminal velocity. Further, the accurate knowledge of raindrop shape has long been an important parameter in cloud physics research due to its immediate application in radar meteorology where it is involved in prediction of rainfall rate with dual-polarized radars [Siliga and Bringi 1976; Bringi and Chandrasekar, 2004].

The factors contributing to the equilibrium shape of a raindrop falling in air at its terminal velocity are the surface tension, hydrostatic, aerodynamic and electrical forces and the forces due to internal circulations inside the raindrop. Balance of these forces determines the shape and stability of the falling drop. Raindrops smaller than 1mm in diameter maintain almost spherical shape as surface tension force in case of such drops is the most dominating force acting on them. In case of large drops, hydrostatic and aerodynamic forces are stronger and make the drops oblate spheroidal shape with a smooth curvature at upper pole and a flattened base at lower pole. This curvature asymmetry increases with increase in drop-size. The shape of the distorted drop is determined by the axis-ratio defined as the ratio of largest vertical and horizontal chords (minor and major axis) of the drop. Importance of the shape of raindrops in the field of cloud microphysics has been recognized since extensive wind tunnel studies of Lenard (1904) who observed drop deformation and speculated the role of surface

tension and its internal circulation on drop shape. Following these initial experiments, several studies carried out with the improved experimental techniques, provided comprehensive information about the role of different forces which determine the shape and stability of the falling drops [Blanchard, 1950; Jones, 1959; Pruppacher and Beard, 1970; Richards and Dawson, 1971; Rasmussen et al., 1985; Kamra and Ahire, 1989; Beard and Kubesh, 1991; Coquillat and Chauzy, 1993; Szakáll et al., 2009; Bhalwankar et al., 2015].

Several theoretical models have been developed to describe the equilibrium shape of oblate spheroidal raindrops, specifically considering the response to gravity [Green, 1975; Beard, 1984], the perturbation response to aerodynamic pressure [Savic, 1953; Pruppacher and Pitter, 1971] and the large amplitude response to both hydrostatic and aerodynamic pressures modified for distortion [Beard and Chuang, 1987]. These models calculate the shape of non-oscillating raindrops. In the atmosphere, however, raindrops continuously oscillate in an oblate-prolate mode. The cause of the oscillations has mostly been attributed to the drop's vortex shedding in the drop wake [Beard et al., 1989b; Saylor and Jones, 2005], turbulence and wind shear [Beard and Tokay, 1991], and collisions with other tiny drops [Johnson and Beard, 1984]. The frequency and amplitude are the key parameters of oscillations of the drop. The equation for the frequency of drop oscillations was first given by Rayleigh (1879) and showed that the drop's oscillation frequency decreases with increase in its size. Moreover, a number of laboratory studies and aircraft measurements confirmed that raindrop oscillations must be the primary cause to attain non-equilibrium shapes and shift in its axis ratio [Jones, 1959; Chandrasekar et al., 1988, Pruppacher and Klett, 2010]. Recent comparisons of mean drop shape and the axis-ratio distribution between the measurements made using 2D video disdrometer and wind tunnel experiments by Thurai et al. (2009) show an increase in oscillation amplitude with increasing drop diameter. All these studies are conclusive that the drops do oscillate and account for the upward shift in the mean axis ratio relative to their equilibrium shapes. Such shift in axis ratio can significantly alter the differential radar reflectivity (Z_{DR}) signals used to estimate the drop size distribution and rainfall rate [Seliga and Bringi, 1976], especially in heavy rain showers. An extensive review involving a variety of theoretical modeling and experiments on behavior of raindrops can be found in literature [Pruppacher and Klett, 2010; Jones et al., 2010; Szakáll et al., 2010].

Besides collision and coalescence, drop breakup is another important process in development of rain in warm clouds [Langmuir, 1948]. It limits the maximum size of the raindrops, controls the growth of raindrops by collision-coalescence process and thereby affects the evolution of the size distribution of raindrops in clouds. Several experiments and theoretical

studies emphasize the collision-induced breakup process as the overwhelming cause of drop breakup [McTaggart–Cowan and List, 1975; Low and List, 1982a, b; Feingold et al., 1988; McFarquhar, 2004a; Testik and Barros, 2007; Testik, 2009; Emersic and Connolly, 2011, Szakáll et al., 2014]. However, it is well known that raindrops larger than a critical size are hydro-dynamically unstable and breakup spontaneously into smaller fragments [Blanchard, 1949; Magarvey and Taylor, 1956; Komabayasi, 1964; Beard and Pruppacher, 1969; Kamra et al., 1991; Reisin et al., 1998].

The third conceivable disruption cause for the drop breakup is the strong electrical forces acting on the drops. In thunderclouds, raindrops carry electric charge and quite often are located in intense electric field. Consequently, the drop charge and electric field produce electrostatic forces on the surface of the drop. These electrostatic forces on the raindrops primarily oppose the surface tension force and affect the balance of other forces acting on drop, resulting in change in their shape and terminal velocity and thus affect the cloud microphysical processes.

The behavior of water drops in strong electric fields has been a subject of several theoretical and experimental simulation investigations. Theoretical models [Brazier-Smith, 1971; Chuang and Beard,1990; Coquilat and Chauzy, 1993, 1994; Coquilat et al., 2003] and laboratory simulation experiments [Macky,1931; Ausman and Brook,1967; Abbas and Latham,1969; Richards and Dawson,1971; Griffiths and Latham,1972; Rasmussen et al.,1985; Kamra and Ahire,1989; Kamra et al.,1991, 1993; Coquillat et al., 2003; Bhalwankar and Kamra, 2007] confirm the distortion of drops due to electrical forces. These studies also show that the strong electric fields deform a water drop to the extent that its surface with high curvatures becomes hydrodynamically unstable and the drop disrupts and/or produces corona discharge. In most of the studies, direction of electric field is considered to be vertical in direction, since on a large scale, the ambient electric field in thunderclouds is predominantly vertical in direction [Fitzerald and Byers, 1962; Marshall and Rust, 1991]. However, it is reported that the electric field inside active thunderclouds are frequently inclined from vertical direction, especially in storms with large stratified regions [Krehbiel et al., 2000]. It is worth noting in this respect that the maximum electric field of 430 kVm^{-1} measured in thunderclouds has been observed to be horizontal in direction [Winn et al., 1974].

Emissions of air pollutants have led to a significant loading of atmosphere from anthropogenic sources in the industrial era. Besides radiative effects, impact of anthropogenic pollutants on cloud microphysical processes have become increasingly important as these elevated aerosols pollute the cloud drops by the nucleation and scavenging processes and

influence the cloud microstructure and precipitation-forming processes in clouds [Ackerman et al., 2000]. Moreover, incidences of acid rain in big cities show a great impact of pollutants on cloud and raindrops. Analysis of rain water and cloud water samples show that there is a variety of chemical compounds in the rain water and their concentrations at different locations vary over many orders of magnitude [Huff and Changnon, 1973; Pruppacher and Klett, 2010]. Impacts of electrical forces on the other forces that govern the drop's morphology differ with the type and amount of drop pollutants.

To improve the knowledge of cloud and rain processes and to find the relevant parameterizations for cloud-microphysical processes, laboratory experiments are essentially important. Moreover, such experiments provide reliable input parameters for the model simulations and provide the necessary data to verify theoretical models with repeated measurements under well-controlled conditions. For example, collision, coalescence and breakup of raindrops are assumed to be main parameters in controlling the evolution of raindrop size distributions. Initially, drop-size distributions were determined from laboratory measurements conducted more than 30 years ago [McTaggart–Cowan and List, 1975; Low and List, 1982a]. Based on results of these measurements the relevant parameterizations have been derived [Low and List, 1982b; McFarquhar, 2004a]. Thus, there is need for more field observations and laboratory experiments with improved techniques to understand the fundamental rain processes. In addition to airborne and ground-based measurements [Chandrasekar et al., 1988; Tokey and Beard, 1996; Thurai and Bringi, 2005; Thurai et al., 2009], several laboratory facilities to simulate the cloud processes like cloud chambers, fall shafts, free-fall tubes, drop levitators and open and close ended vertical wind tunnels are now available [Pruppacher and Klett, 2010 and references therein].

A small, low turbulence, open-ended vertical wind tunnel was designed, constructed and developed at IITM, Pune to study the microphysical processes in controlled conditions close to the real atmosphere [Kamra et al., 1986]. Water drop of a few millimeter sizes can be freely suspended for sufficiently long time in vertical air stream of the wind tunnel and subjected to different electrical stresses similar to those prevailing in clouds. Basic consideration in designing this vertical wind tunnel is to create a velocity profile wherein a drop could be suspended in the air-stream with minimum turbulence. Several experiments were conducted in our wind tunnel, especially to demonstrate the significance of the electrical forces acting on the drop surface in determining the shape and other characteristics of the water drop.

2. The vertical wind tunnel facility at IITM

The IITM vertical wind tunnel consists of a centrifugal blower driven by a 186W motor which sucks the air from an air-conditioned room and maintains the continuous airflow in the divergent section. Figure 1 shows a schematic diagram of the wind tunnel.

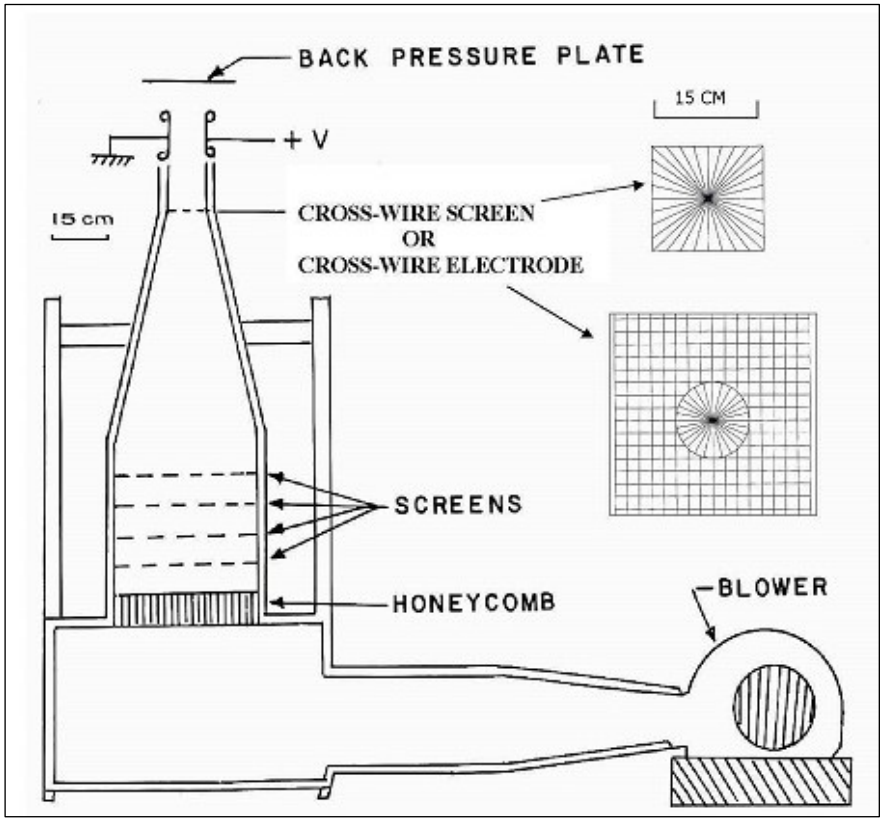

Figure 1. *A schematic diagram of a vertical wind tunnel and the cross-wire screens used to create a velocity well*

A wire mesh screen of size 8 meshes per centimeter was fixed between the blower and divergent section to streamline the incoming air. The air slowly expands and enters into a 84 x 80 x 40 cm reservoir which smooths out the fluctuations in the airflow. From the reservoir, air travels vertically up in to a straight section of cross-section 40 x 40 x 50 cm fitted with one honey-comb made from 7.5 cm long cells of 0.6 x 0.6 cm cross-section and four screens of wire-mesh of size 8 meshes per centimeter to minimize the turbulence in the airflow. Above the straight section there is a converging section which reduces the tunnel cross- section from 40 x 40 cm to 12 x 12 cm at its top over a vertical length of 66 cm which compresses and smoothens the airflow. A test-section of 12 x 12 x 15 cm cross-section made of Perspex is placed above the convergent section. In between the convergent section and test-section is placed a crossed-wired mesh screen made from a 0.25 mm copper wire. It

slightly lowers the vertical air stream velocity in the center of the test-section and thus creates a velocity-well where a drop could be suspended. To maintain the velocity-well up to some distance above the crossed-wire screen, a back pressure plate of 30 x 30 cm cross-section placed above the test-section of the tunnel. This plate exerts a back pressure on the air stream by deflecting the airflow outwards and prevents the collapse of the velocity-well. The effect of changing the height of back pressure plate on the time of suspension of drops before their escape from the air stream was studied. It was observed that placing the back pressure plate at a height of 22 cm above the test-section of the wind tunnel was most suitable for suspension of drops. With this setup, a water drop could be suspended for many minutes in the velocity-well created by crossed-wire screen.

A technique has been developed for the simultaneous suspension of multiple drops [Kamra and Ahire, 1985]. In place of crossed-wire screen, another screen made with wire of 30 SWG can be fitted in the tunnel to simultaneously suspend five drops of approximately same size [Figure 2]. Study of such equal size drops colliding along their horizontal or major axis, especially under the effect of electrical forces may be of interest for cloud and rain processes.

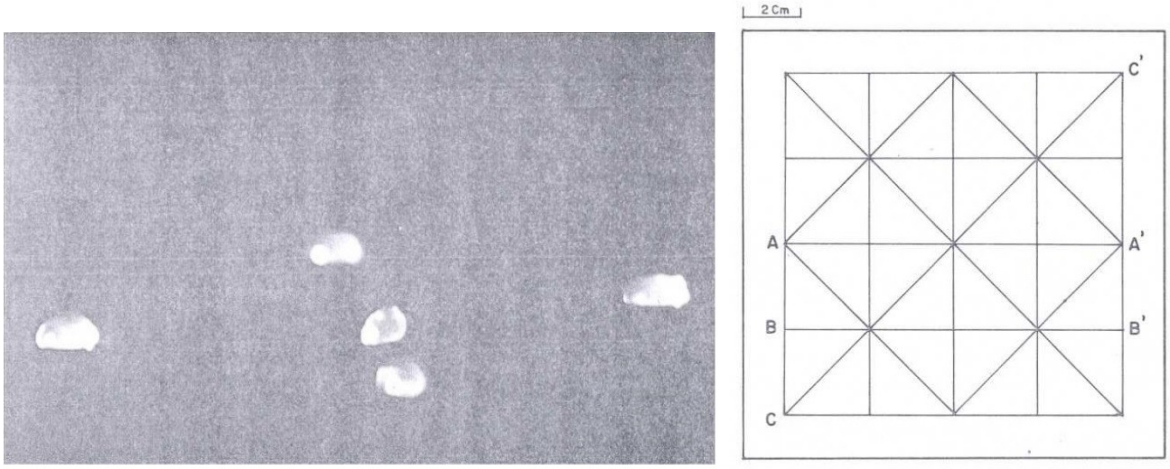

(a) (b)

Figure 2. (a) *Photograph of five water drops suspended above the test section of the wind tunnel, (b) Screen made of a brass frame and 30 gauge (0.25 mm) copper wire.*

2.1 The vertical velocity and turbulence measurements

The vertical velocity and intensity of turbulence of the airflow in the cross-section of the wind tunnel are the fundamental parameters to achieve the greater stability of the drops. Both the parameters were measured accurately with **a** pre-calibrated Velocical-multi-function ventilation meter (TSI model 9564-P). It can measure the average velocity with a resolution

of 0.01 ms^{-1} and calculates the intensity of turbulence from a 3-minute sample of velocity reading in a particular position. The measurements showed that the vertical velocity up to ~12 m/s could be achieved in the test-section of the tunnel. The intensity of turbulence was found to be less than 0.65 % in the center of the tunnel up to a height of 10 cm above the top of the test-section where the drops were suspended. For maintenance of the velocity-well up to some distance a back pressure plate is placed at a height of 22 cm above the test section of the wind tunnel. With this setup, drops of 6.6 mm diameter could be suspended for many minutes before their escape with some transient eddy or fluctuations in the airstream. Drops > 6.6 mm in diameter were mostly forced to escape from the airstream due to their breakup. It was observed with this setup that a drop of liquid paraffin could be suspended for many hours in the airstream. Utilizing this facility several experiments were conducted by freely suspending the charged/uncharged water drops of known diameters to understand the effect of electrostatic forces on the raindrop morphodynamics.

3. Observational techniques and variables used in experiments

3.1 Drop diameter

In our experiments, distilled water drops of 2.67 to 8.2 mm equivalent diameters were suspended in the wind tunnel at their terminal velocities using a calibrated pipette (Single channel Finnpipette-F2, Thermo Fisher Scientific Inc., USA) with 0.2 ml volume accuracy. This drop size range covers the typical raindrop size as well as the larger raindrops observed in the melting band in cold clouds or in the rain shaft region formed below the melting large ice pallets and snowflakes.

3.2 Drop charge and electric fields

To electrically charge the drops, a wire connected to a power supply was inserted into the pipette. Voltage to which the wire was raised was so adjusted that water drops were charged with positive charges of q = 0, $5\,X\,10^{-11}$C, $5\,X\,10^{-10}$C. The value of charge $5\,X\,10^{-10}$C is very high and found only on a small number of drops located in the intensely electrified regions of thunderstorms. However, the value of $5\,X\,10^{-11}$C is a better representative value of drop charge in clouds.

To create a vertical electric field (E_V), a flat circular aluminium plate of 38 cm diameter and 1.2 cm thickness with suitably rounded edges is mounted above the test section. This plate acts as a positive upper electrode as well as the back-pressure plate. The lower

electrode is 25 x 25 cm in size and made of iron wire-mesh of size 8 meshes per inch a hole of 5 cm diameter at its center. A cross-wire screen made of 40 SWG copper wire is fitted in this hole and it creates the required velocity-well for suspending water drops. The cross-wire screen is replaced with this electrode in the experiments to study the effect of the vertical electric field. Lower electrode is fitted between the diffuser and test sections. The upper electrode is connected to a high-voltage power supply of 0 – 100 kV and lower electrode is grounded. Vertical distance between these two electrodes is 16 cm. With these arrangements, no measurable corona was observed from the electrodes even when the potential of upper electrode is raised upto 80 kV.

To generate the horizontal electric field (E_H), two flat circular electrodes of 15 cm diameter and made out of 2.2 cm thick aluminium plate are fabricated and mounted vertically above the test-section. The edges of the electrodes are suitably rounded and smoothened to increase the corona threshold. The two electrodes are separated by 12 cm from each other. One of the electrodes is connected to a dc power supply of 0 to 100 kV and the other one to the ground. Raising the potential of either electrode upto 60 kV is not observed to produce any measurable corona from the electrodes. Thus an electric field of upto 500 kVm^{-1} can be generated between the electrodes.

To compare the influences of the direction of electric fields, horizontal and vertical electric fields of magnitude 0, 100 kVm^{-1}, 300 kVm^{-1} and 500 kVm^{-1} were used in our experiments. Electric field greater than 300 kVm^{-1}, though on the higher side of the large-scale fields observed in thundercloud, may exist in small regions of the intensely electrified thunderstorms.

3.3 Chemical impurities

In most of the laboratory experiments, drops of distilled water were used to study their distortion. However, it is well known that the polluted air over the industrial regions or over the big city areas can significantly pollute the raindrops. Consequently, raindrops are contaminated with the aerosol particles and trace gases. Specific experiments were performed by suspending the polluted water drops to study the combined effect of electric field and pollutants on drop's distortion. Drops were polluted with 100 ppm solution of Sulfate salt (ammonium sulphate) and Nitrate salt (potassium nitrate) as these pollutants are commonly observed with significant impact on the atmosphere [Hegg et al., 1994; Sanusi et al., 1996] and were subjected to different values of the horizontal electric fields.

4. Methodology

In our experiments, water drops of different diameters were suspended in the wind tunnel at their terminal velocities using a calibrated pipette. The pipette was connected to power supply with a wire to electrically charge the water drops. The calibration of the electric charges and the corresponding voltage required was done outside the wind tunnel using Keithley electrometer. Similar values of voltage were used while introducing drops of required size and charge in the wind tunnel. For uncharged drops wire connected to the pipette was grounded. The time period from suspension to breakup (life-time) of a drop was measured with a stop watch. To study the drop size distribution, the fragments of water drop after its breakup were collected on Whatman filter paper (number 1) coated with methylene blue dye. A calibration curve used by Blanchard (1953) was used to convert spot diameter into drop diameter.

To study the behavior of water drops in electric field, uncharged drops of various sizes were released by calibrated pipette and suspended between the electrodes in absence of electric field. Then the electric field was quickly raised (~ in 2 to 3 sec) to a desired value. This decay time eliminates the residual oscillations caused by the generation of drop while detaching from the pipette and is sufficient to compensate the effect of such oscillations with the viscous forces in the drop [Lamb, 1945, Beard, et al. 1991]. The time interval from when the electric field was raised to its desired level to its spontaneous breakup or escape from the air-stream termed as suspension time was measured with a stop watch. The residing time of water drops in the electric field is long enough to cover its natural oscillations.

4.1 Imaging technique

To understand the physical mechanism of the microphysical processes, a potential technique in laboratory experiments is to take photographs of the process at regular intervals. Over the period of more than three decades of experimentation in our wind tunnel, the photographic technique has been continuously improved and updated to get higher resolution and sharper images.

In our earlier experiments, snapshots of oscillating water drops were captured with a still camera with 1 photograph per 60 sec. Later, a 16 mm movie-camera with a speed of 48 frames per sec (i.e. 20 ms resolution) was used to record the temporal variations of a drop's shape during different phases of its oscillation. A high-power projection DC lamp was used to illuminate the drop with both dark field and bright field background. After developing the films from this camera, the drop-shape and axis-ratio variations were measured using a

microscope. However, the lower speed of photography used in these experiments was still not enough to cover all modes of oscillation of smaller drops, which are known to oscillate at much higher frequency than larger drops.

A more sophisticated system comprising a 10-bit CMOS chip based, high speed monochrome camera (Mega Speed MS55K, Canadian Photonic Labs Inc.) with a maximum resolution of 1280 X 1020 pixels and variable frame rate from 25 to 1000 frames per second was used in our later experiments for acquiring real-time video data. This allowed the continuous recording of the high-quality images of the suspended drops with high resolution for relatively long time. It can also record the temporal shape variations of the oscillating drop and cover the higher modes of oscillation of the drops. The pixel size of the camera chip is 12 μm and a lens with magnification of 1:2 was attached to the camera so that a spatial pixel resolution of 24 μm was obtained during the measurements.

In order to get high contrast, the drops were illuminated with a 300 W DC cold light lamp creating bright-field background. Diffused uniform illumination was maintained by placing a milk-glass plate in between the light source and the drop. Using this set-up, image of a drop appears as a dark object on a bright background, providing a suitable high contrast for further image analysis. Water drops of different sizes were photographed with 1000 frames per second to obtain a series of drop oscillations. Since the camera has inbuilt 16 GB memory, it can store 23 seconds data with the above speed and resolution.

Drops were photographed after 2-3 sec of their detachment from the pipette to eliminate the residual oscillations caused by the generation of drop while detaching from the pipette [Lamb, 1945, Beard, et al. 1991]. According to formula given by Lamb (1945), the viscous relaxation time (τ) for fundamental mode of oscillation for a drop of 6.6 mm diameter is estimated to be 2.1 sec. This decay time provides an upper limit and is sufficient to compensate the effect of such oscillations with the viscous forces in the drop [Pruppacher and Klett, 2010]. Figure 3 (a and b) shows the photograph of the vertical wind tunnel with vertical and horizontal electric field arrangement respectively with a high speed camera positioned and water drop suspended in horizontal electric field.

(a) **(b)**

Figure 3: (a) *Photograph of vertical wind tunnel horizontal electric field arrangement with a high speed camera, (b) water drop suspended in wind tunnel in presence of horizontal electric field.*

4.2 Image processing and data analysis

After each experimental run, the uncompressed AVI files recorded with high speed camera were manually cropped in such a way that the images of the oscillating drop remain within the cropped region. Since the AVI files were in uncompressed format, it provides raw image data with maximum precision in image quality. These recorded 10-bit images are required to be processed to get sharp black and white images to precisely determine the major and minor axis of the drop. 'Image J', a public domain Java image processing and analysis software was used for this purpose. It can read images in AVI format and can display, edit, analyze, process, save and print images. It supports standard image processing functions such as contrast, sharpening, smoothing, edge detection.

As a first step of the analysis, the 10-bit gray-level images of the drops from the cropped file were converted to B-W images using the image threshold adjustment. The threshold value (i.e. the value above which all pixels were set to white and below which were set to black) was determined by the software using an algorithm that converted the gray-scale image to binary version [Jones and Saylor, 2009]. In the present experiment, the threshold average value was 76. Thus, the images of drops obtained appeared as dark objects on a bright diffused background, resulting in high contrast between drop and background. Out-of-focus images were not considered for further processing. Later, the region of interest (ROI) was selected as an elliptical shape, including the entire drop in the first image of a recorded series and adjusted such that the drop will remain oscillating within the selected elliptical area for the whole series. In the next step, all the images were analyzed by the software to get major (2a) and minor (2b) axis of the drop from which axis ratios (b/a) were computed. These steps of image processing and analysis are shown in Figure 4. In determining the major and minor axes, the uncertainty appears from the edge detection. With a spatial pixel resolution of 24 μm, for a 2-pixel size inaccuracy, the magnitude of the major and minor axes can be determined with 48- μm accuracy and a relative error of ~ 4% is estimated for the axis ratio determination in our measurements

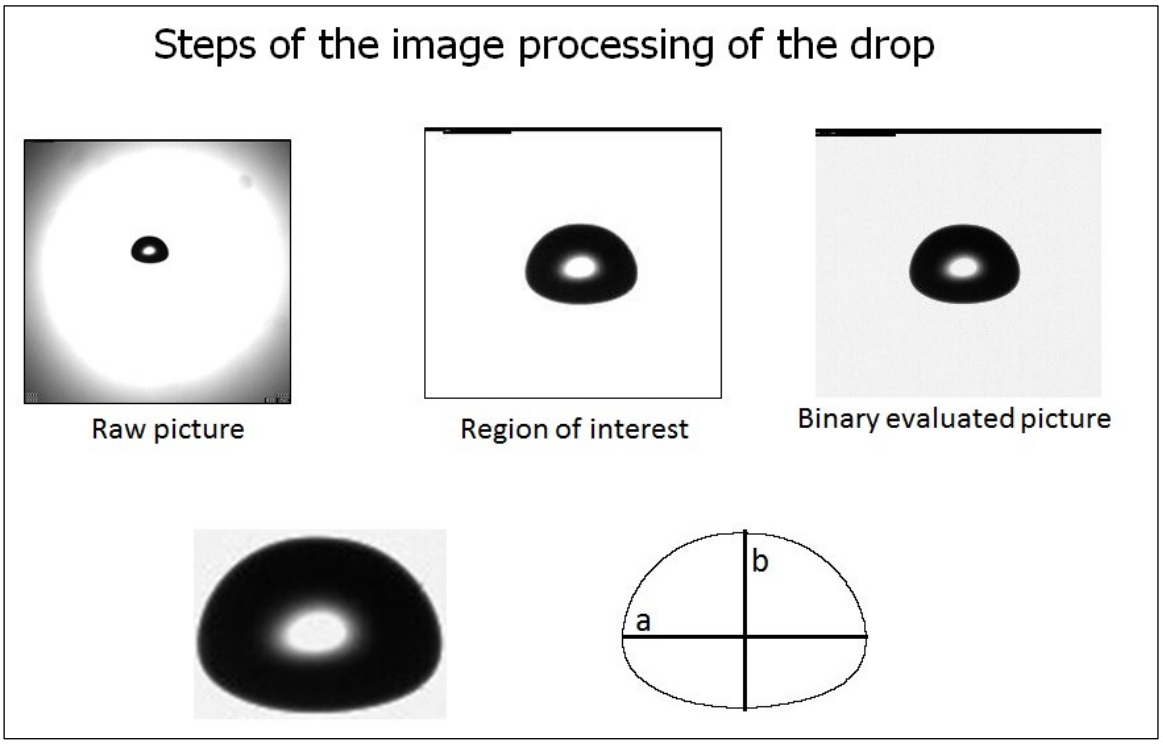

***Figure 4**: Steps of image processing and analysis of semi-major (a) and semi-minor axis (b) to calculate the axis ratio of a drop.*

5. Studies conducted in the vertical wind tunnel over the last three decades

For more than three decades, our vertical wind tunnel has been utilized in various experiments to study the distortion, oscillations and spontaneous breakup of charged and uncharged, polluted and non-polluted water drops of millimeter size in presence and absence of electric field. In different experiments conducted to study the effect of the vertical, horizontal or no electric field, the drops have the unique advantage of being suspended in the same experimental set-up. Moreover, unlike in earlier studies the drops are suspended at their terminal velocity and spend sufficient time in electric field to undergo many oscillations about their equilibrium shape while they are exposed to the electric field. Our emphasis in these studies has been to investigate the effects of electrical forces on drop's behaviour. These studies are summarized below.

i. Shape and oscillations of the water drops freely suspended in a horizontal electric field,
ii. Comparison of the deformation of drops between the vertical and horizontal electric field configurations,
iii. The onset of disintegration and corona discharge from water drop surface in the horizontal electric field,
iv. Distortion of polluted and unpolluted water drops in the horizontal electric field,
v. Role of drop distortion in enhancing the lightning activity in clouds formed over cities,
vi. Spontaneous breakup of charged and uncharged water drops and the size distribution of droplets after breakup,
vii. Spontaneous breakup of polluted drops in horizontal electric field,
viii. Evaporation of charged and uncharged water drops,
ix. The breakup modes of the water drops in the presence of the horizontal electric field.

6. Results

Major results obtained in our simulation experiments, conducted in the IITM vertical wind tunnel are summarized below. Detailed results and their implications in cloud physics are described in various publications referred therein:

6.1 Shape and oscillation of drops in presence /absence of electric fields

Accurate determination of raindrop shape and oscillation is an important factor in radar meteorology and provides information for better understanding of the drop collision-coalescence and breakup processes in clouds. Raindrops are defined to have minimum diameter of 100 μm [Pruppacher and Klett, 2010]. Although, typical raindrops have diameter between 1 and 3 mm, large drops of upto 8 mm have been observed in field measurements

[Beard et al., 1986]. These large raindrops are formed either from colliding drops resulting in coalescence during their free fall or by melting of the falling large ice pallets and snowflakes in mixed-phase clouds. Drops smaller than 1 mm in diameter maintain almost spherical shape when freely falling through the air. However, drops larger than 1 mm in diameter exhibit oblate shape because other forces become progressively stronger in comparison to the surface tension force. The ratio of semi-minor (b) to semi-major (a) axis of the drop, known as axis ratio, is the simplest quantitative indicator of drop shape and distortion.

For investigating the shape and oscillations of the drops, experiments were conducted by freely suspending distilled water drops of equivalent diameter ranging from 2.67 to 6.6 mm in the vertical wind tunnel and subjected to the vertical / horizontal electric field of 0, 100, 300 and 500 kV cm^{-1}. Sufficiently large data (3000 to 23,000 images) on the drop shape were collected by photographing the drops, initially using a 16-mm movie camera in our earlier experiments and more recently using a high-speed camera [Bhalwankar and Kamra, 2007; Balwankar et al., 2015]. From series of photographs, time-averaged axis ratios and oscillation frequencies of drops of different sizes were determined. Figure 5 shows the change in the drop's axis ratio with its diameter in absence or presence of vertical / horizontal electric field strength of 0, 100, 300, and 500 kV m^{-1}. A comparison of various curves in the figure effectively demonstrates the stretching and elongation of the drop in the direction of electric field. Decrease in axis ratio with the increasing drop size is observed for all values of electric field due to increasing aerodynamic and hydrostatic forces and decreasing surface tension forces with the drop size. However, as compared with the case when E = 0, while the vertical electric field decreases the oblateness and tends to make the drop more spherical and then prolate, the horizontal electric field keeps increasing the oblateness of the drop and progressively enhance the elongation of the drop along its major axis. The observation well illustrates the fact that both aerodynamic and electrostatic distortions act together in a horizontal electric field but counteract in a vertical electrical field. The lower value of instability field required in a horizontal than in a vertical field is most probably because of the fact that unlike in the vertical electric field, any enhancement in the horizontal electric field keeps elongating the drop along its major axis which eventually leads to its instability during its oscillating motion. Moreover, the horizontal electric field and flattening of the water drop feedback each other for mutual enhancement and the drop distortion in each oscillation may not be limited to the fixed values of ambient field on the drop surface [Kamra et al., 1993].

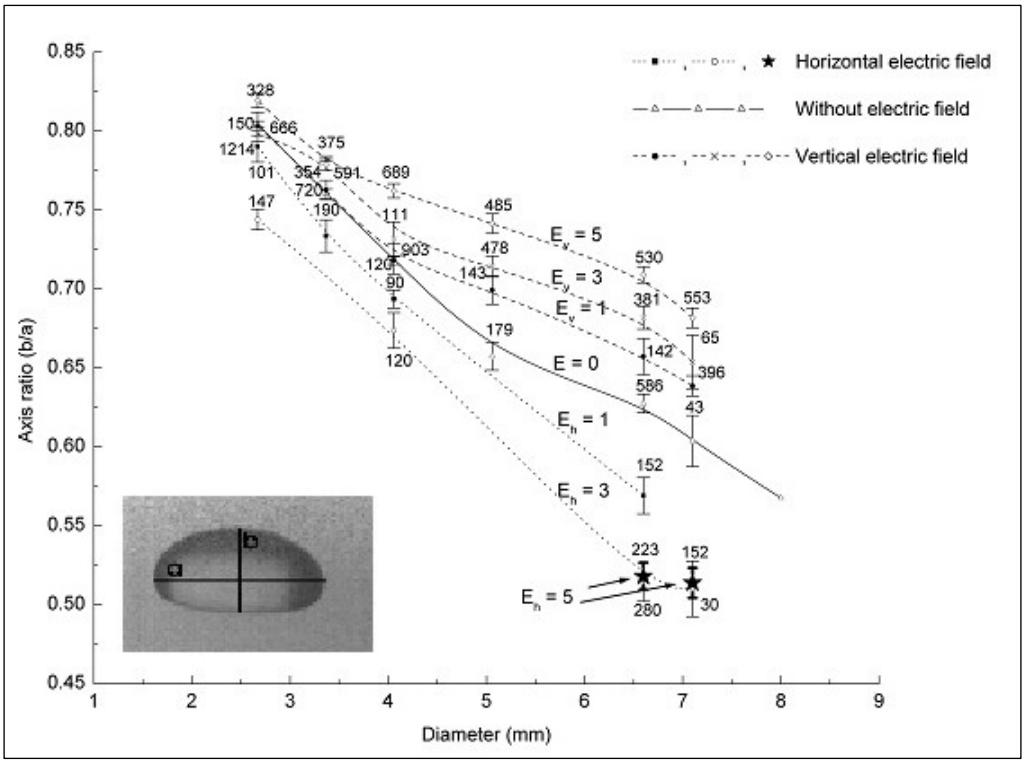

Figure 5. *Change in axis ratio (b/a) with drop diameter in absence and presence of horizontal/vertical electric field strength of 0, 100, 300 and 500 kVm^{-1}. All values of the vertical and horizontal electric field, Ev and Eh, respectively, are in kV cm^{-1}. Number on the top of all error bars indicate the number of frames used for calculating the average values. Also inserted a photograph of a drop showing semi-major (a) and semi-minor (b) axis.*

Raindrops in clouds are known to continuously oscillate in the oblate-prolate mode about their equilibrium axis-ratio and these oscillations account for an upward shift in the estimated average axis-ratio values [Beard, 1984; Chandrasekar et al., 1988; Beard and Kubesh 1991, Szakáll et al. 2009]. The key parameters to quantify the drop's oscillations are their frequency and amplitude. In the present study, the oscillation frequency of drops of diameter $2.67 \leq d \leq 6.6$ mm in the horizontal electric field of 0, 100, 300, and 500 kV m^{-1} was determined from the temporal variations of the axis ratio computed from the continuous images of water drops using a high-speed camera [Bhalwankar et al. 2015]. Figure 6(a) illustrates different phases of drop shape of a suspended water drop of equivalent diameter 5.11 mm showing one oscillation period of 35 ms. Although, a systematic decrease in oscillation frequency with drop size is observed in no electric field values, there is no significant change in the oscillation frequency with electric field even when the horizontal electric field increased as high as 500 kV m^{-1} (Figure 6b).

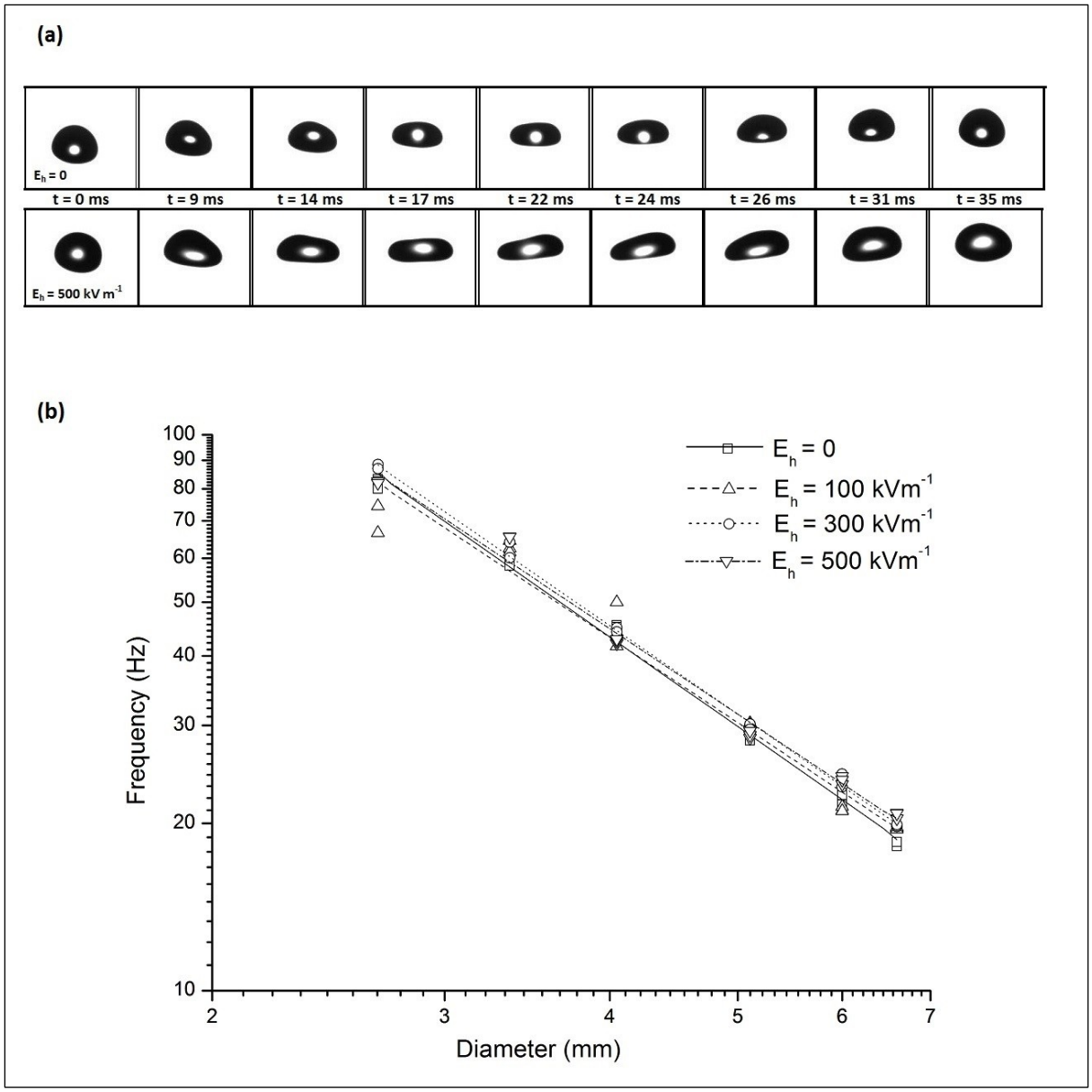

Figure 6. *(a)Typical photographs of suspended water drop of 5.11 mm diameter illustrating one oscillation period in horizontal electric field of 0 and 500 kVm^{-1}. Time (t) of the images is also shown for both series (b) Oscillation frequencies of drops in absence and presence of horizontal electric field of 100, 300, and 500 kVm^{-1}.*

It is well-known that the oscillations in falling drop set-in in drops larger than 1 mm in diameter. The smaller drops oscillate with very high frequency, but very small amplitude [Pruppacher and Klett, 2010]. However, the amplitude rapidly increases with drop size and may lead to instability and eventual breakup of the drop. Thus, the magnitude of oscillation is the key parameter in the growth and breakup processes of water drops. The amplitude (A) of simple harmonic oscillator is related to the standard deviation of drop oscillation (σ) as $A = \sqrt{2}\ \sigma$. Detailed computation of oscillation amplitude for drops considered in our

experiment in absence/presence of electric field is given in Bhalwankar et al., 2015. Figure 7 shows variations in oscillation amplitude with diameter of various drops in the absence and presence of horizontal electric fields. Curves for electric field ≤ 300 kV m^{-1} show that the amplitude of oscillation systematically increases with the increase in drop size and then tends to flatten-off from some threshold value of the drop diameter up to d = 6 mm. However, in higher electric field of 500 kV m^{-1} the increase in the amplitude of oscillation with drop diameter continues up to d = 6.6 mm. Further, the oscillation amplitude decreases with the increase in electric field for a particular drop diameter. Moreover, the Fast Fourier Transform (FFT) analysis of series of drop images revealed that the oblate-prolate oscillations of drop, primarily caused by the fundamental mode (2,0) of oscillations exist for all drops in the size range of 2.67 ≤ d ≤ 6.6 mm both in the absence or presence of a horizontal electric field. Moreover, in addition to this fundamental axisymmetric mode, a (2,1) mode develops for smaller drops of 2.67 mm and 3.36 mm diameter and a (2,2) mode develops for drops larger than 5.11 mm diameter.

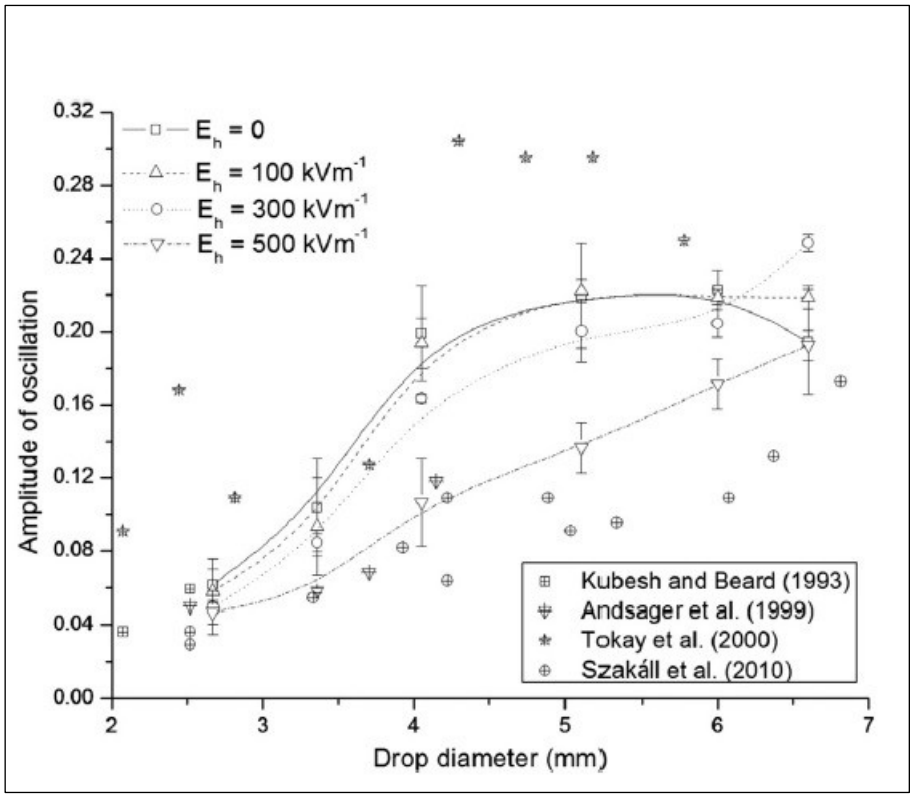

Figure 7. *Variations in amplitude of oscillations with drop diameters in absence and presence of horizontal electric fields with error bars. Symbols represent mean values of the amplitude. Earlier experimental results of Kubesh and Beard (1993), Andsager et al. (1999), Tokay et al. (2000) and Szakáll et al. (2010) are also plotted.*

6.2 Evaporation of charged and uncharged water drops

Knowledge of the growth and evaporation of water drops within the cloud and during their fall in sub-cloud layer is important in understanding the mechanisms of the precipitation formation. An experiment was performed to study the effect of ventilation on the rate of evaporation of the millimeter sized ($1.9 \leq D \leq 4.1$ mm) charged ($q = 10^{-10}$ C) and uncharged water drops suspended in the vertical wind tunnel [Bhalwankar et al., 2004]. The linear relationship,

$$f_v = 0.907 + 0.282\ X \tag{1}$$

observed between the mean ventilation coefficient, f_v, and a non-dimensional parameter X, ($X = N_{Sc,v}^{1/3} N_{Re}^{1/2}$ where $N_{Sc,v}$ is Schmidt number and N_{Re} is Reynold's number) is in agreement with the results of Pruppacher and Rasmussen (1979) for uncharged water drops. However, in case of charged drops carrying 10^{-10} C of charge, this relationship gets modified to

$$fv = 0.4877 + 0.149\ X \tag{2}$$

Results show that the rate of evaporation of charged drops is slower than that of uncharged drops of the same size (Figure 8).

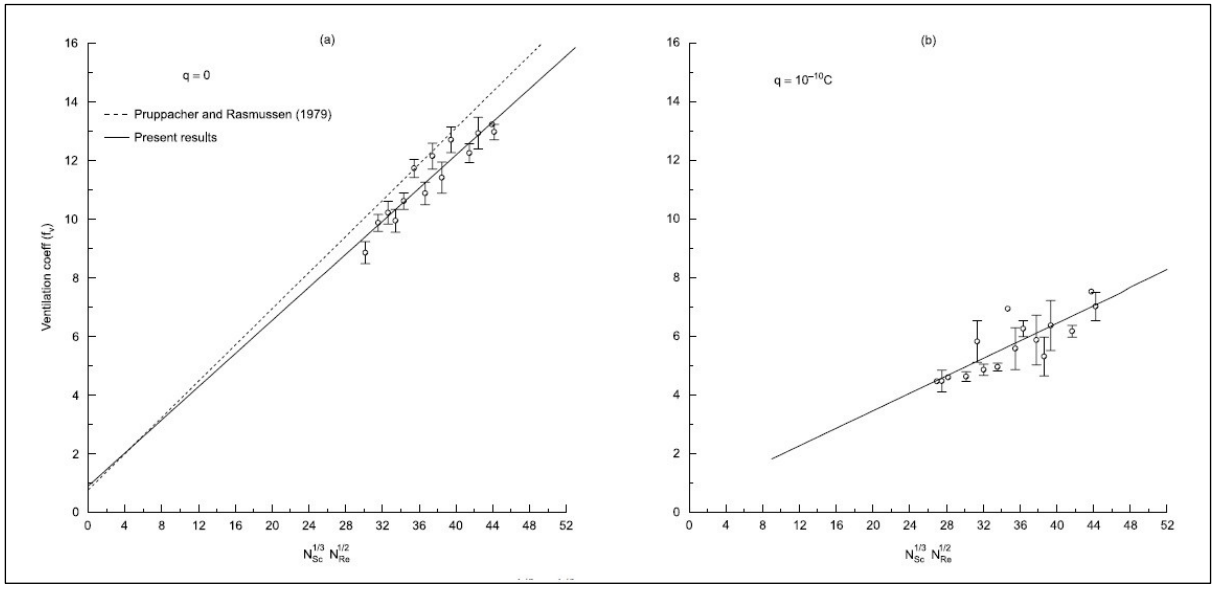

Figure 8. *Variation of ventilation coefficient with $N_{Sc}^{1/3}\ N_{Re}^{1/2}$ and drop radius (a_0) for* ***(a)*** *uncharged drops, and* ***(b)*** *charged drops.*

Further, the calculations derived from experimental results of Kinzer and Gunn (1951) showed that the ventilation coefficient f_v is related with a dimensionless ventilation factor F as $f_v = 1 + F (N_{Sc,v} N_{Re} / 4\pi)^{1/2}$. They found that F is a marked function of square root of Reynold's number (N_{Re}) of the drop. Our present results of the dependence of F on $(N_{Re})^{1/2}$ for charged and uncharged drops are compared with results of Kinzer and Gunn (1951) and Beard and Pruppacher (1971) in Figure 9.

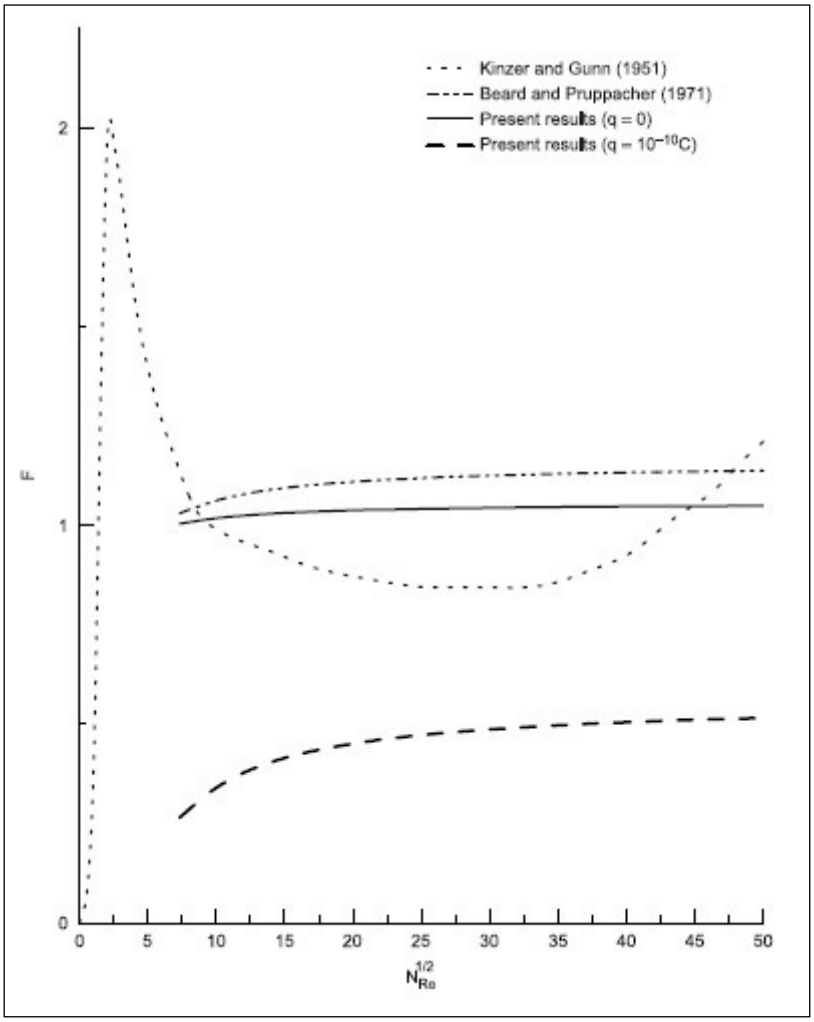

Figure 9. *Dependence of ventilation factor, with the square root of Reynold's number for charged and uncharged drops*

The variations in our experimental values of F with $(N_{Re})^{1/2}$ are comparable with those of Beard and Pruppacher (1971), for uncharged drops. Beard and Pruppacher (1971) pointed out that Kinzer and Gunn (1951) set the drop temperature equal to the ambient wet bulb temperature which might be somewhat higher than the equilibrium surface temperature. Moreover, they derived values for the rate of change of mass from the variation in fall speed

of an evaporating drop using double finite difference method and used inaccurate values for the drag on a drop. It may introduce error in calculating F values in their computations and the error will be larger for the smaller drops. The values of F are much lower for the drops carrying a charge of 10^{-10}C than that for the uncharged drops. Such highly charged drops develop a pronounced oblate distortion caused by the charge density enhancement at their waist, [Kamra et al., 1991; Chuang and Beard, 1990]. This change in shape of the charged drops alters the airflow around them and consequently results in a decrease in their ventilation coefficients.

The present results can be applied to compute the evaporation of raindrops falling from clouds through the sub-saturated sub-cloud air of various relative humidities in a NACA standard atmosphere. Following Mason (1952) and using an iterative method, we have computed the size of drops falling below the cloud in air of various humidities and reaching the ground with a radius of 1 mm and the results are illustrated in Figure 10.

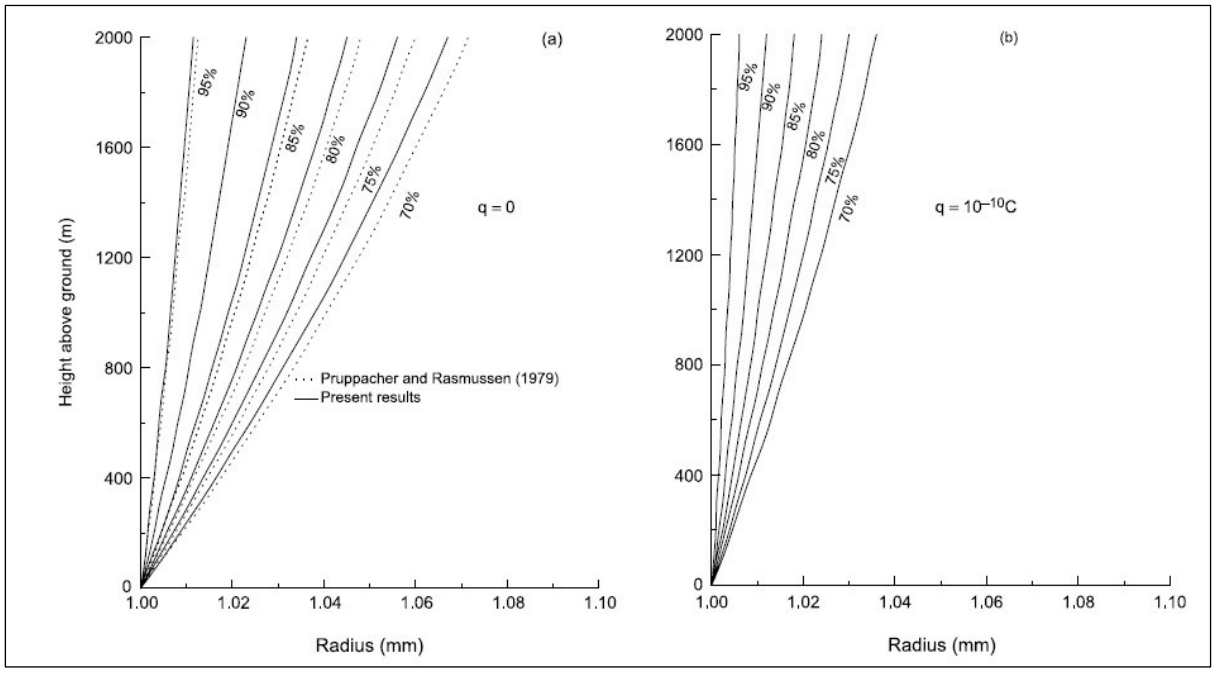

Figure 10. *Change in size an (a) uncharged drop, and (b) charged drops falling below a cloud through the subsaturated air of various relative humidities in NACA Standard Atmosphere to arrive at the ground with the radius of 1 mm.*

Results show that the lower the relative humidity of the sub-cloud air the larger the drop has to be to reach the ground with a given size. It follows from Figure 10 that the charged drops leaving the cloud base have to be smaller in size than the uncharged drops.

Oscillations of the drop and the change in airflow around drops are suggested to contribute to lowering of the ventilation coefficients for charged drops. The relaxation time required for a ventilated drop to reach its equilibrium temperature increases with the drop size and is higher for the charged than for the uncharged drops. It is concluded that in a given distance, charged drops will evaporate less than that of uncharged drops.

6.3 Effect of electrical forces on spontaneous breakup of water drops

Drop breakup may be the result of a spontaneous breakup due to aerodynamic and hydrodynamic instability of a large single drop or a collision of drops which causes collision-induced breakup [Blanchard, 1950; Komabayasi et al., 1964; Low and List, 1982b]. Recently, Villermaux and Bosa (2009) observed that the spontaneous breaking of drops into smaller fragments containing whole spectrum of sizes observed in rain is accomplished within a timescale shorter than the typical collision time between the drops in rain. However, the overwhelming cause of the drop breakup in clouds is believed due to the collisions with smaller drops [Low and List, 1982b]. In addition to above two causes the strong electrical force acting on the surface of drops located in the high ambient electric field regions of a thundercloud is another possible factor affecting the drop breakup. In thunderclouds, raindrops carry electric charge and quite often are located in intense electric field. Consequently, the charges and electric field produce electrostatic forces on the surface of the drop. Magnitude of electrical charge on some drops in the intensely electrified regions of thunderclouds may approach the Rayleigh's limit due to a variety of electrical processes (e.g., Gaskell et al., 1978; Marshall and Winn, 1982).

6.3.1 Spontaneous breakups of charged and uncharged drops

The spontaneous breakup of charged and uncharged drops has been investigated by suspending the drops in the airstream of the vertical wind tunnel. The drops of $6.6 \leq d \leq 8.2$ mm were charged with positive charges of $q = 5 \times 10^{-11}$ C and 5×10^{-10} C and the size distribution of the fragments after the breakup of charged as well as uncharged drops were measured [Kamra et al., 1991]. Results show that probability of spontaneous breakup of a drop increased with size and charge of the drop (Figure 11). This can be qualitatively explained as a result of the enhanced surface charge density around the waist of the oblate shaped drop where the drop has maximum curvature during its oscillation. When the oscillating drop reaches its largest elongation, the surface charge density also attains its maximum value at the maximum curvature of the drop. Consequently, the contribution of outward acting electric force increases as the drop deforms.

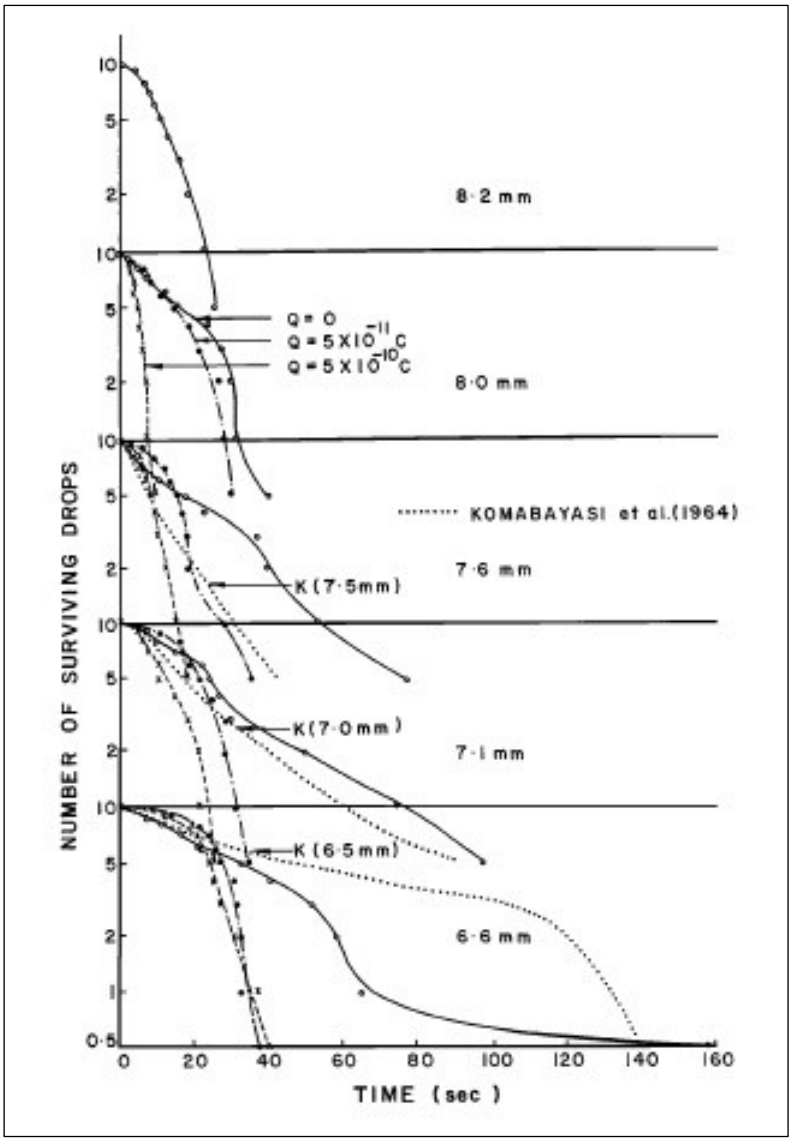

Figure 11. *Number of charged and uncharged water drops surviving spontaneous breakup at different times. On the logarithmic scale of ordinate the point is plotted at 0.5 instead of zero*.

So the surface charge and flattening of the drop feedback each other for mutual enhancement. Thus the net effect of the charge on the drop is to elongate the width of its base. As a result, a standing wave on the bottom surface of the drop will amplify and cause the drop to break up if the width of the drop base is $d \geq \lambda_c/2 = 0.855$ cm where $\lambda_c = 1.71$ cm is the critical wavelength above which waves on the bottom surface of the drop are unstable [Komabayasi et al., 1964]. This increased cross-sectional area of the charged drop is exposed to the airflow which in turn increases the drag and thus decreases the terminal velocity of the drop [Dawson and Warrender, 1973; Gay et al., 1974; Chuang and Beard, 1990; Coquillat

and Chauzy, 1993]. Distortion of the charged drops to enhanced oblateness with respect to the uncharged drops further increases the probability of their breakup.

Spontaneous breakup of water drops can be considered as a random occurrence. Therefore, as in case of radioactive matter, the time at which the number of surviving drops remains half of the initial value, can be considered as half-life of the drop. Figure 12 shows that half-life of the drop decreases with the size of the drop and that this decrease is sharper when the drop is electrically charged. It is interesting to note that half-life of the drops carrying charge of 5 x 10^{-11} C is closer to the half-life of uncharged drops when drops are of 8 mm size and closer to that of water drops carrying charge of 5 x 10^{-10} C when the drops are of 6.6 mm size. This again points out to the importance of surface charge density in determining the stability of the water drops.

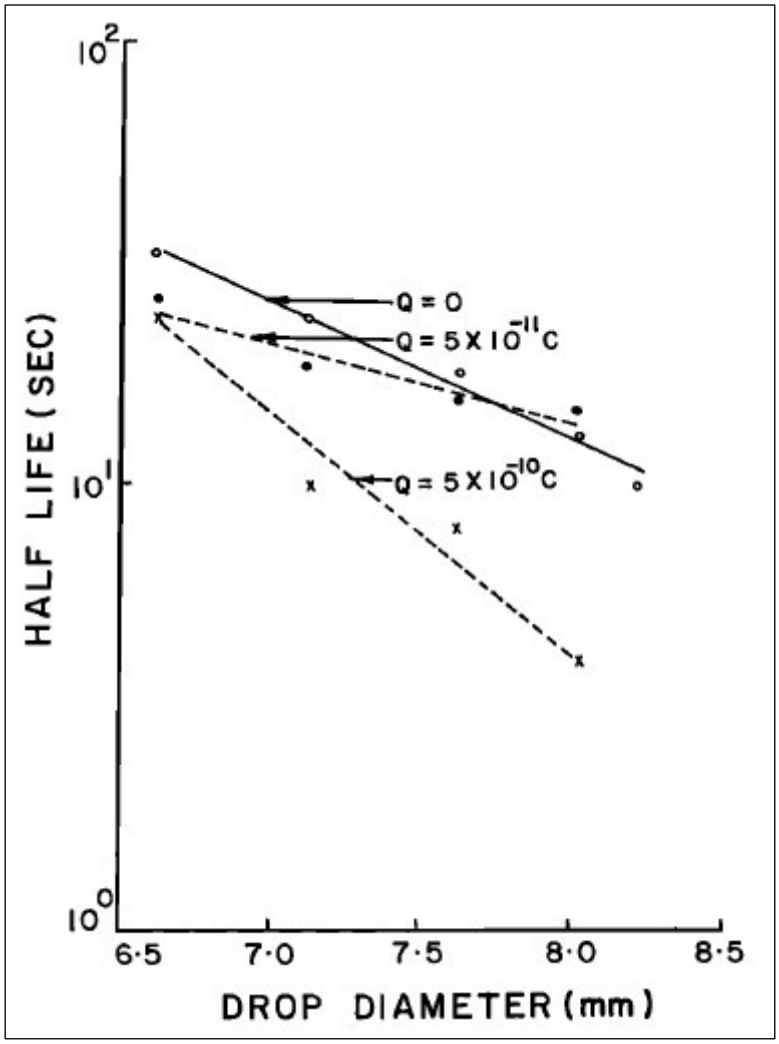

Figure 12. *Half-life of charged and uncharged water drops of different sizes.*

In addition to half-life, the average life (the time when cumulative number of drops remain 1/e of the initial value) and the probability of breaking of drop (inverse of the average life) for charged and uncharged drops of different sizes. As the size of the drop or its charge increases, half-life and average life of the drop decreases and probability of its breaking increases. If τ_h is the half-life in seconds and diameter D is in millimetres, data can be expressed by the following empirical formulae:

For uncharged drops,

$$\tau_h = 4.402 \times 10^3 e^{-0.733D}, \qquad D \geq 6.6 \text{ mm} \tag{3}$$

For charged drops with $Q = 5 \times 10^{-11}$ C,

$$\tau_h = 3.822 \times 10^2 e^{-0.417D}, \qquad D \geq 6.6 \text{ mm} \tag{4}$$

For charged drops with $Q = 5 \times 10^{-10}$ C,

$$\tau_h = 5.533 \times 10^4 e^{-1.185D}, \qquad D \geq 6.6 \text{ mm} \tag{5}$$

The average life τ sec can be computed from

$$\tau = 1.44 \tau_h \tag{6}$$

and the probability of breaking p s^{-1} from

$$p = 1 / \tau \tag{7}$$

The size distribution of fragments in each 0.4 mm width of diameter after spontaneous breakup of parent drops of different size has been calculated. The following empirical formulae are obtained to represent the monotonous decrease in size distribution of droplets resulting from breakup of the charged and uncharged drops.

For uncharged drops,

$$N(D)\,\delta D = 1.54 \times 10^{-2} D_0^3 e^{-0.453 D}\,\delta D \tag{8}$$

For drops charged with $Q = 5 \times 10^{-11}$ C,

$$N(D)\,\delta D = 1.06 \times 10^{-2} D_0^3 e^{-0.349 D}\,\delta D \tag{9}$$

For drops charged with $Q = 5 \times 10^{-10}$ C,

$$N(D)\,\delta D = 0.47 \times 10^{-2} D_0^3 e^{-0.186 D}\,\delta D \tag{10}$$

where $N(D)\,\delta D$ is the number of droplets in the range of diameter between D mm and $D + \delta D$ mm and the D_o is the diameter of the parent drop in millimetres.

Moreover, the total number of droplets produced by spontaneous breakup of drop, increases with size of the parent drop and it is more if the drop is uncharged than that if it is charged. However, the number of droplets larger than a critical size is more if the parent drop is charged and the number of droplets smaller than that critical size is more if the parent drop is uncharged (Figure 13).

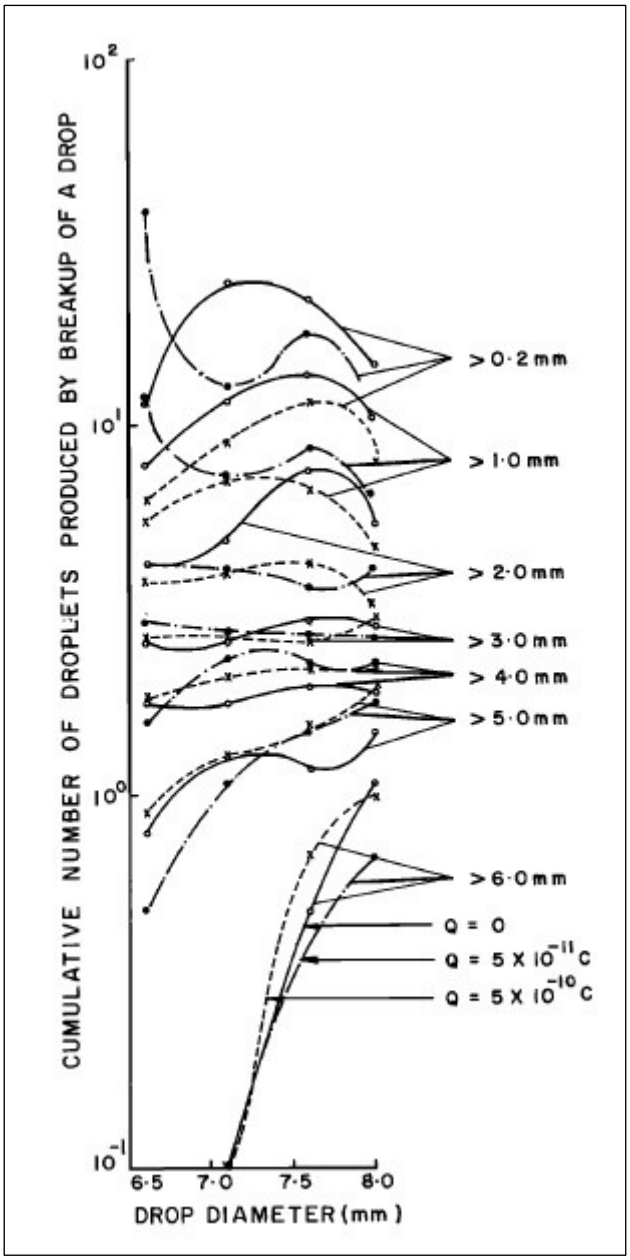

Figure 13. *Cumulative number of fragment droplets produced on spontaneous breakup of charged and uncharged water drops of different sizes.*

6.3.2 Spontaneous breakup of drop in absence / presence of horizontal electric field

Both theoretical and experimental studies show that water drops falling in a strong electric field elongate along the direction of field due to interaction of the field and the polarization charges induced on the drop. If the field strength exceeds a certain critical value the drop becomes unstable and finally disintegrates. Experiments were performed in our wind tunnel to understand the effect of horizontal electric field (E_H) on drop breakup process and onset of corona discharge from water drops [Kamra et al. 1993]. Uncharged water drops of 4.5 to 8 mm diameter were suspended in the wind tunnel in presence of horizontal electric

field E_H = 0, 100, 300, 400, 500 kV m^{-1} and photographed with a 16 mm movie camera at 48 fps. Figure 14 shows the percentage of the number of drops < 6.6 mm diameter that breakup when they are suspended in E_H = 300, 400 or 500 kV m^{-1}. It is worth noting that while no drop of diameter <6.6 mm breaks up in absence of an electric field, 90% of 6.3 mm drops and 20 % of 5 mm drops break up in an electric field of 500 kV m^{-1}. Even in an electric field of 300 kVm^{-1}, 20% of the drops of 6.3 mm diameter break up.

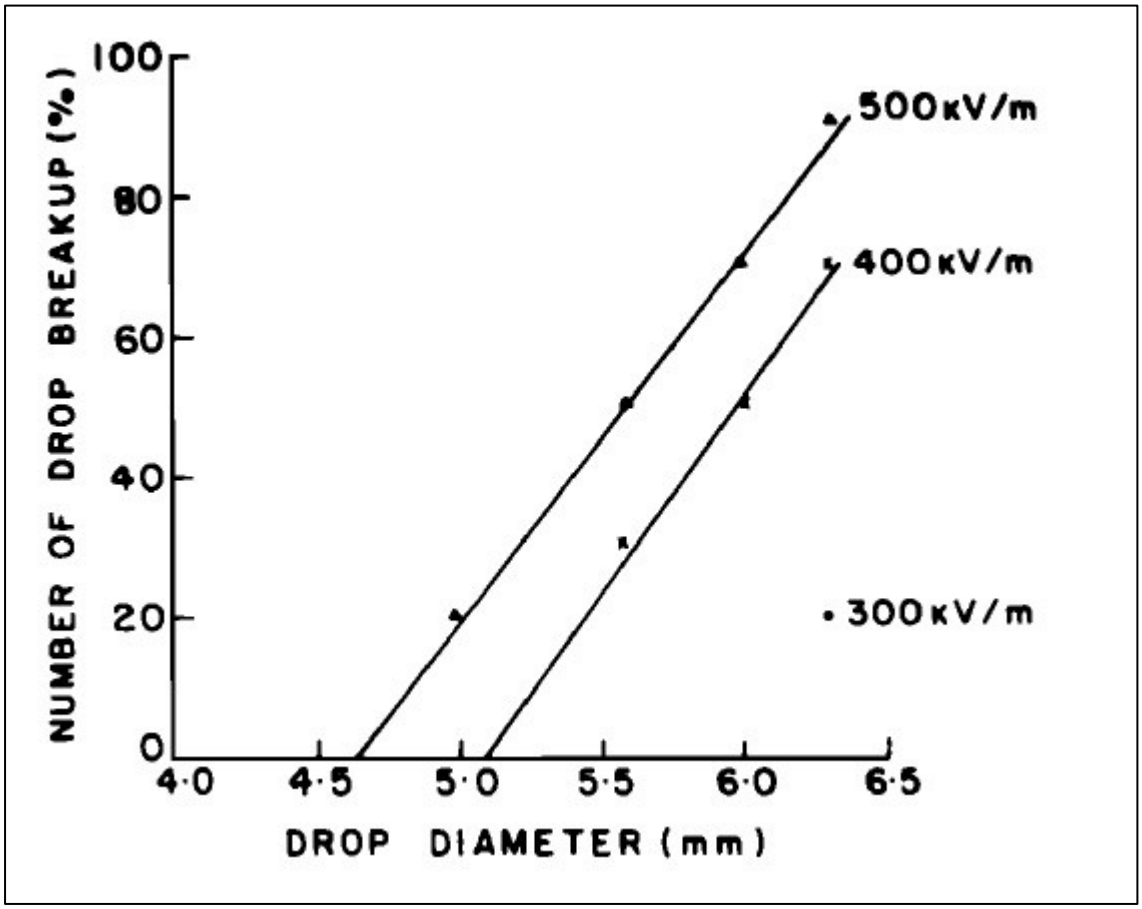

Figure 14. *Percentage of number of uncharged drops of different diameters that break up in different horizontal electric fields.*

Figure 15 shows half-life (as defined in sec 6.3.2) for uncharged drops of different diameters in presence or absence of horizontal electric fields. The half-life of the drop decreases with the increase in the drop size or the electric field. Half-life of a drop decreases approximately by an order of magnitude when it is exposed to a horizontal electric field of 500 kV/m. If τ_h is the half-life in seconds and diameter D is in millimetres, the data for different values of horizontal electric field F_H in Figure 15 for drops of D < 6.6 mm can be expressed by the following empirical formulae:

$$\tau_h = 1.93 \times 10^3 e^{-0.48D}, \qquad F_H = 0 \text{ kV/m} \tag{11}$$

$$\tau_h = 1.67 \times 10^3 e^{-0.66D}, \qquad F_H = 300 \text{ kV/m} \tag{12}$$

$$\tau_h = 3.822 \times 10^2 e^{-0.417D}, \qquad F_H = 400 \text{ kV/m} \tag{13}$$

$$\tau_h = 0.74 \times 10^3 e^{-0.70D}, \qquad F_H = 500 \text{ kV/m} \tag{14}$$

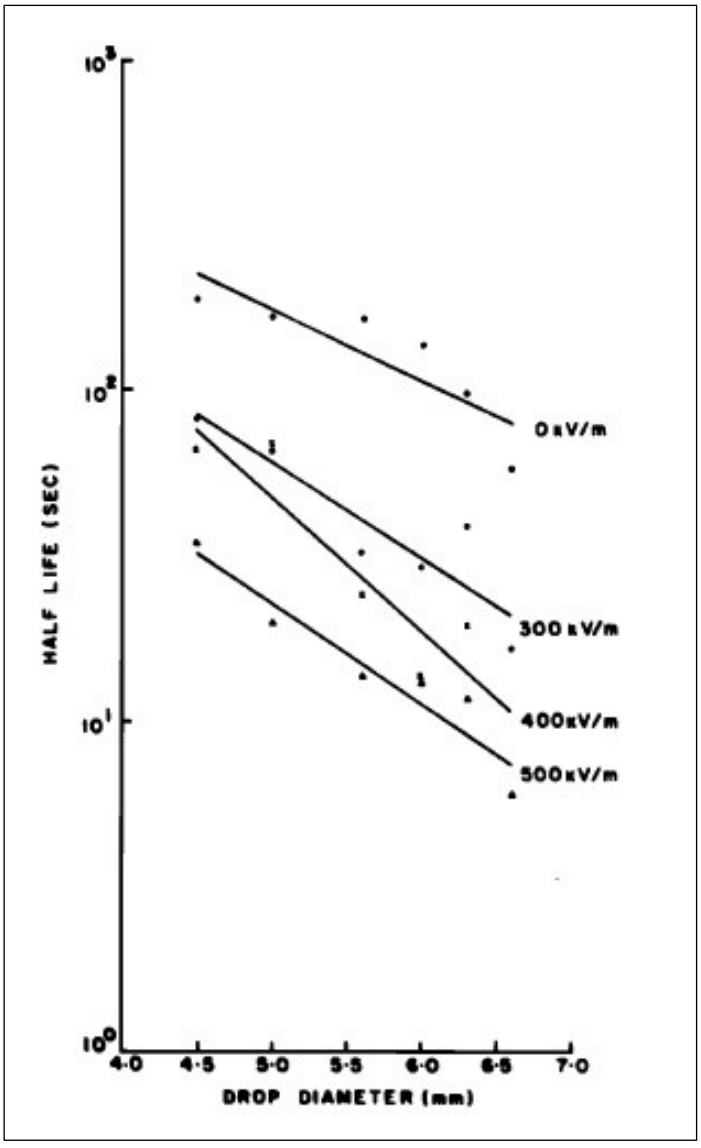

Figure 15. *Half-life of uncharged water drops of different sizes in different horizontal electric fields.*

6.3.3 Instability criterion

A large water drop suspended in a wind tunnel oscillates and rotates as an ellipsoid around its vertical minor axis. So, when the orientation of the maximum amplitude of the horizontal axis of the drop coincides with the direction of the horizontal electric field, elongation of drop is maximum. In this position the drop will be most unstable and will have maximum probability of breakup. To observe the values of instability field for drops of different diameters, we suspended the drops in the wind tunnel and kept increasing the value of electrode potential in steps of approximately 2 kV every second, and the value of potential at which the drop breaks up is noted. Figure 16 shows the values of instability field for different drop sizes. From these observations, the criterion for instability for water drops of diameter $5 \leq D < 6.6$ mm freely suspended in presence of horizontal electric field can be expressed as

$$F_H (r_0/\sigma)^{1/2} = 0.98 \pm 0.03 \text{ (in esu)} \qquad 6.6 \text{ mm} \geq D \geq 5.0 \text{ mm} \tag{15}$$

where F_H is the horizontal electric field in esu, r_0 is the drop radius in cm and σ is the surface tension in dyne/cm. Figure 16 also show the curve for Taylor's instability criterion of water drops in vertical electric field [Taylor, 1964].

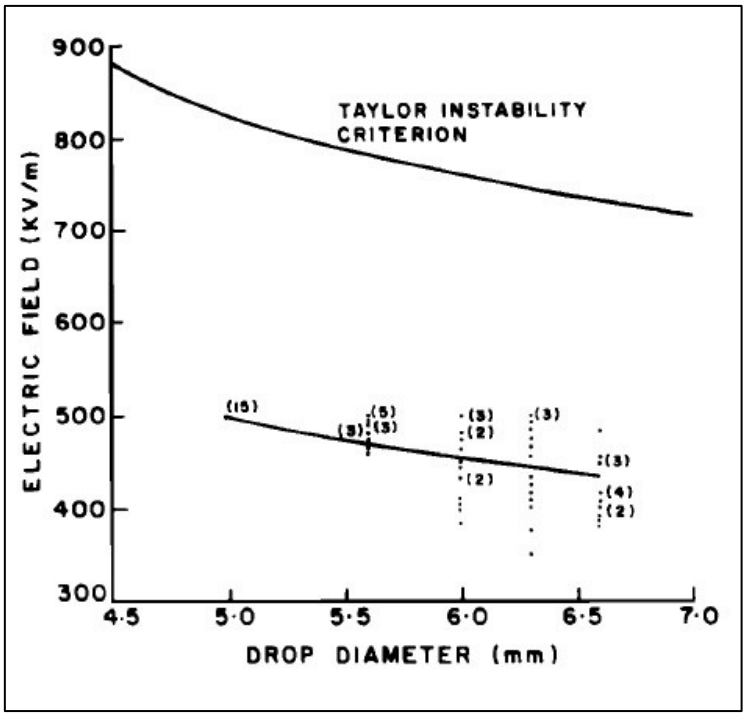

Figure 16. *Dependence of instability field on drop diameter for uncharged drops freely suspended and on drop diameter exposed to horizontal electric field and its comparison with the theoretical curve of Taylor (1964). Dots shows the scatter in instability field observed for different drops of the same size and the numbers in brackets show the number of drops that break up at the same value of electric field.*

The theoretical calculations of Taylor (1964) and experimental measurements [Nolan, 1926; Macky, 1931; Griffith and Latham, 1972] where the drops were falling through an intense vertical electric field region observed the values of instability constant as 1.61, 1.51, and 1.81 respectively. The lower values of instability field observed in our experiments can be understood by considering different conditions in our experiment as compared to previous studies. In earlier theoretical studies, the electric field is assumed as vertical and oscillations of the drop are mostly ignored by considering it as a static drop of spherical shape. Moreover, in most of previous experimental studies, the drops are exposed to the vertical electric field for a very short time, so they may not experience many oscillations and the maximum elongation due to electrical forces. Under vertical electric field conditions the electrical force has to work against the aerodynamic and hydrodynamic force acting on the drop. So the electric field required to destabilize the shape of the drop has to be larger in such cases than that in the case when the electric field is horizontal. On the other hand, in our experiment the drop oscillates in presence of horizontal electric field throughout the period of its suspension to undergo many oscillations about its equilibrium shape. So the probability of its plane of oscillation coinciding with the direction of horizontal electric field during one of its oscillations is comparatively very large in our experiment. In this position of the maximum elongation, the drop will be most unstable and develop sharp edges which may produce corona even in the lower values of electric field if the local field on the drop surface is sufficiently enhanced.

6.3.4 Corona discharge from water drops

The electric charge on a water drop and the presence of horizontal electric field around it, deform the water drop to the extent that its surface develops high curvatures and becomes hydrodynamically unstable. The sharp curvatures developed at the drop's ends intensify the electric field around them and thus ionize the surrounding air and produce corona discharge followed by the drop breakup. Photographs in Figure 17 illustrate the sequences of distortion and occurrence of corona discharge occurring from the sharp edge of a 7.1 mm diameter drop and its subsequent breakup.

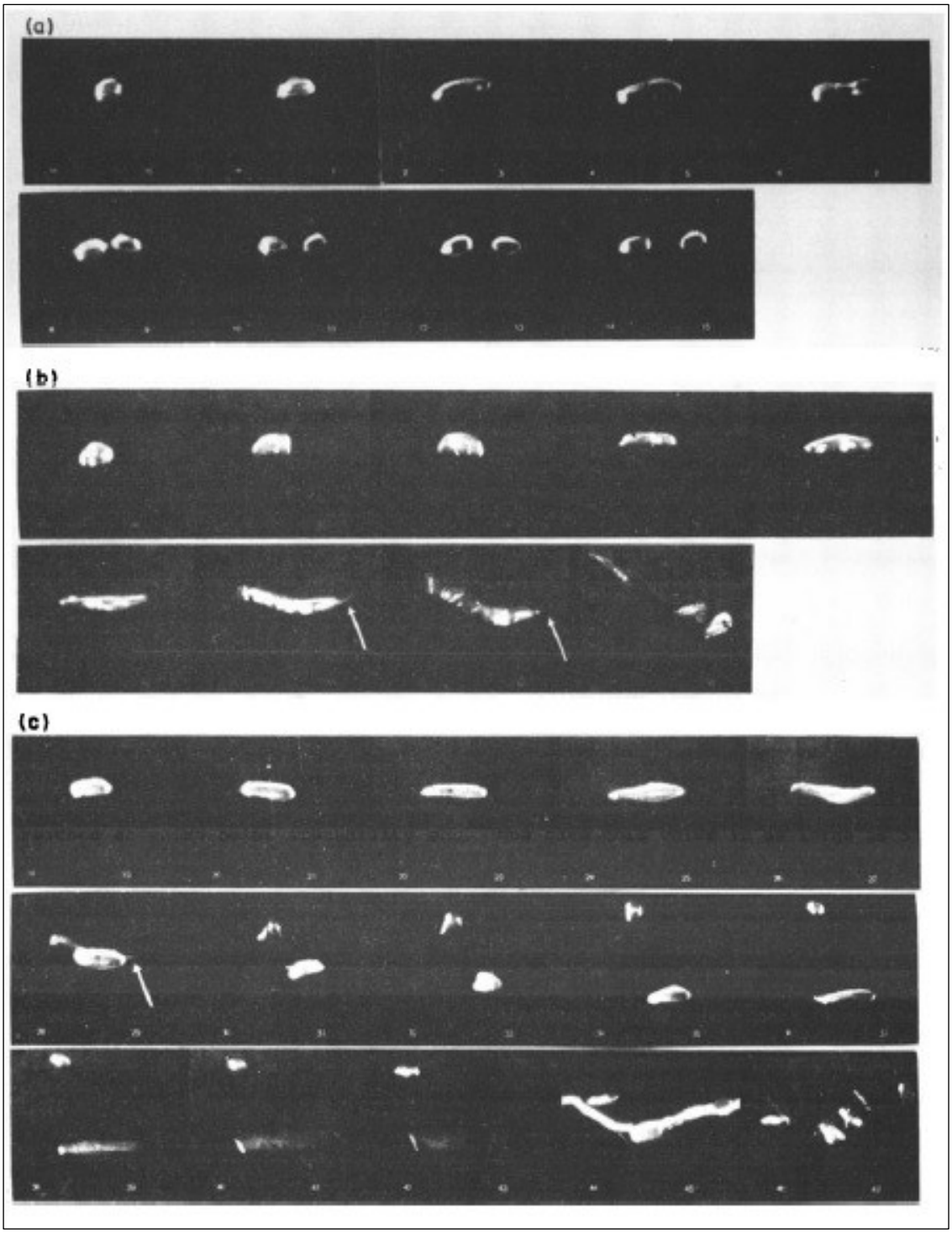

Figure 17*. Photographs of breakup of uncharged drop of 7 mm diameter (a) in absence of electric field, and (b, c) in presence of a horizontal electric field of 500 kV/m. In all figures, time increases from left to right, and successive frames are 21 ms apart. Occurrence of corona from the edge of the drop indicated by arrows can be seen in the seventh and eighth frame of the sequence of Figure 15b and in the sixth frame of the sequence of Figure 15c. Corona in sequence Figure 15c is followed by a bright spark between electrodes in fourteenth frame.*

Besides the dark-field photography, the occurrence of corona from water drops was also detected from static noise in the medium wave in a radio receiver. Most of the drops produce corona just before their breakup. All drops ≥ 7.1 mm produce corona in a E_H = 500 $kVcm^{-1}$. Surprisingly, a small fraction of very large drops of 8.0 mm diameter produced corona even in as low electric field as 200 $kVcm^{-1}$(Figure 18).

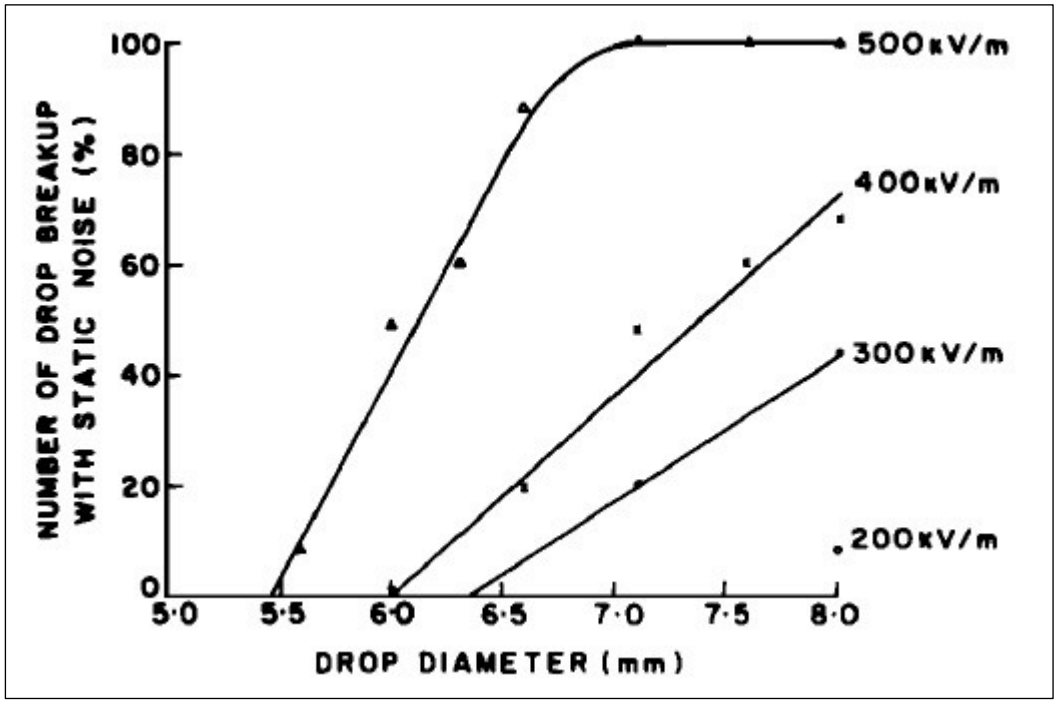

Figure 18. *Percentage of total number of drops producing static noise before their breakup in different horizontal electric fields.*

6.4 Mode of drop breakup in absence / presence of electric field

Mode of drop breakup is important, as the size and number of resulting droplets may considerably differ in each type of breakup. In our recent experiments, the influence of strong horizontal electric field (E_H) on different stages of deformation and eventual breakup of the large water drops of 6.6, 7.0 and 7.25 mm diameter has been studied in the vertical wind tunnel using high-speed photography [Bhalwankar et al., 2017]. As reported in earlier studies, we have also documented dumbbell, filament and bag type of breakup in E_H = 0 [Blanchard, 1949; Komabayasi et al., 1964; Villermaux and Bossa, 2009; Pruppacher and Klett, 2010]. As the drops considered in our experiment are large in size and already deformed, during their oblate-prolate oscillations, they develop a concave depression at upstream side of the drop. Based on the photographic observations, i) dumbbell type of breakup occurs when this concavity deepens at the center of the drop to form a short bridge interconnecting the two

approximately equal sized droplets appearing roughly at the same horizontal plane in the airstream at the time of breakup, ii) In filament type of breakup, the two blobs of the breaking drop are not equal in size. So the smaller blob is carried higher up by the airstream. A long but thin filament interconnecting the two blobs develops in the process. During this process some water may further drain down through the filament from the upper smaller drop to the lower bigger drop, still increasing the inequality in their sizes. Finally, the filament spontaneously breaks up forming two large and a few small droplets, iii) bag type of breakup occurs when a drop progressively flattens and the base develops a concave depression, which explosively deepens and develops rapidly into an expanding bag supported by an annular ring. The breakup occurs when the bag bursts into multiple smaller droplets whilst the annular ring breaks up into few larger droplets. Selected images in Figure 19 display the typical examples of a dumbbell (a), filament (b), and bag (c) type breakups in $E_H = 0$. The time period between the time (t = 0) when the drop's minor axis is maximum at the start of its final oscillation and the time when the drop's first breakup occurs i.e. when the drop first breaks up into two approximately equal size drops, is counted for each drop. Henceforth, we shall call this period as the breakup time of the drop.

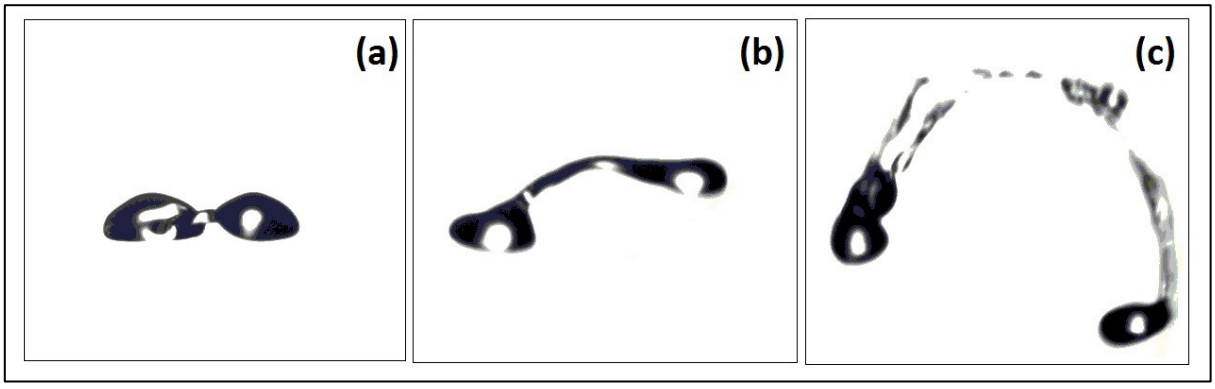

Figure 19. *Typical photographs of suspended water drop of 7.25 mm diameter in the absence of an electric field illustrating (a) dumbbell type, (b) filament type, and (c) bag type breakups.*

In presence of $E_H = 500$ kVm^{-1}, the magnitude of minor axis of the oblate-shaped drop, in its final oscillation is much reduced as the electric force tends to stretch the drop along its major axis to become more flattened and contributes to destabilize the drop. Elongation of the drop is an important factor in the formation of the number and size of the droplets after its breakup. Thus, the length of major axis of the drop in each frame of the last oscillation before its breakup has been measured and the time is determined by the number of frames it takes to attain this shape. The breakup time observed for drops of 6.6, 7.0 and 7.25 mm

diameter in our experiment ranges from 13 - 41 ms in $E_H = 0$, whereas it is 57- 105 ms when exposed to $E_H = 500$ kVm^{-1}. It suggests that the effect of horizontal electrical force ultimately overcomes the balance of other forces acting on the drop in elongating it in the direction of electric field which eventually results in the spontaneous breakup of the drop. Therefore, although the lifetime of the drop since its suspension to breakup is reduced in $E_H = 500$ kVm^{-1} as compared to that in $E_H = 0$ [Kamra et al., 1993], the length of elongation and breakup time of the drop increase in E_H.

6.5 Extreme elongation of drop in presence of horizontal electric field

During our recent experiment to study the breakup modes [Bhalwankar et al., 2017], some water drops experienced very large elongation along their major axis in $E_H = 500$ kVm^{-1}. In this experiment, the bright-field illumination was used for photography as our emphasis was to study the detailed features of the breakup mechanism.

The cases, in which the length of elongated drops under E_H exceeded four times their drop diameters, are henceforth called as cases of extreme elongation. We believe that this happens when the major axis of the distorted drop coincides with the direction of electric field. Since the drop is rotating and oscillating in different modes, probability of such coincidence to happen is small. In our experiment we observed two such cases of extreme elongation. Figure 20 illustrates one such event of the extreme elongation of a drop of 7.0 mm diameter. The drop elongates progressively from its oblate shape (0 ms) to sheet shape (15 ms) and develops the shape of a concavo-convex lens. Soon its concavity is suppressed and is further elongated along the major axis. At its ends, the drop begins to develop sharp curvature (from ~ 60 ms onward) and gets more sharpened with time. Simultaneously, a filament/neck joining two blobs of water is formed in the middle of the drop. At this time, events of fine jet spray of tiny droplets are observed at particular intervals ejected from one sharp end of the drop and each lasted for ~ 2 and 4 ms respectively. Again, another jet is observed at 105 ms from the other sharp end of the droplet and it lasts for ~ 2 ms. Each jet ejects several tiny droplets. These jets are not visible in the print version of the photographs, so a schematic diagram showing these jets is drawn in Figure 20b. During the same period, the filament in the middle of the drop breaks up to separate it into two droplets. Finally, the curvature also produce droplets and the parent drop breaks up at 90 ms. The maximum length of the horizontal elongation of this drop is measured and found to be 29 mm. Although, only two jets were observed in this drop, as many as 4 jets were observed from one end of the drop at a time interval of 8 to 9 ms in case of another drop of 7.25 mm diameter and this drop was observed to elongate upto 42 mm before its breakup.

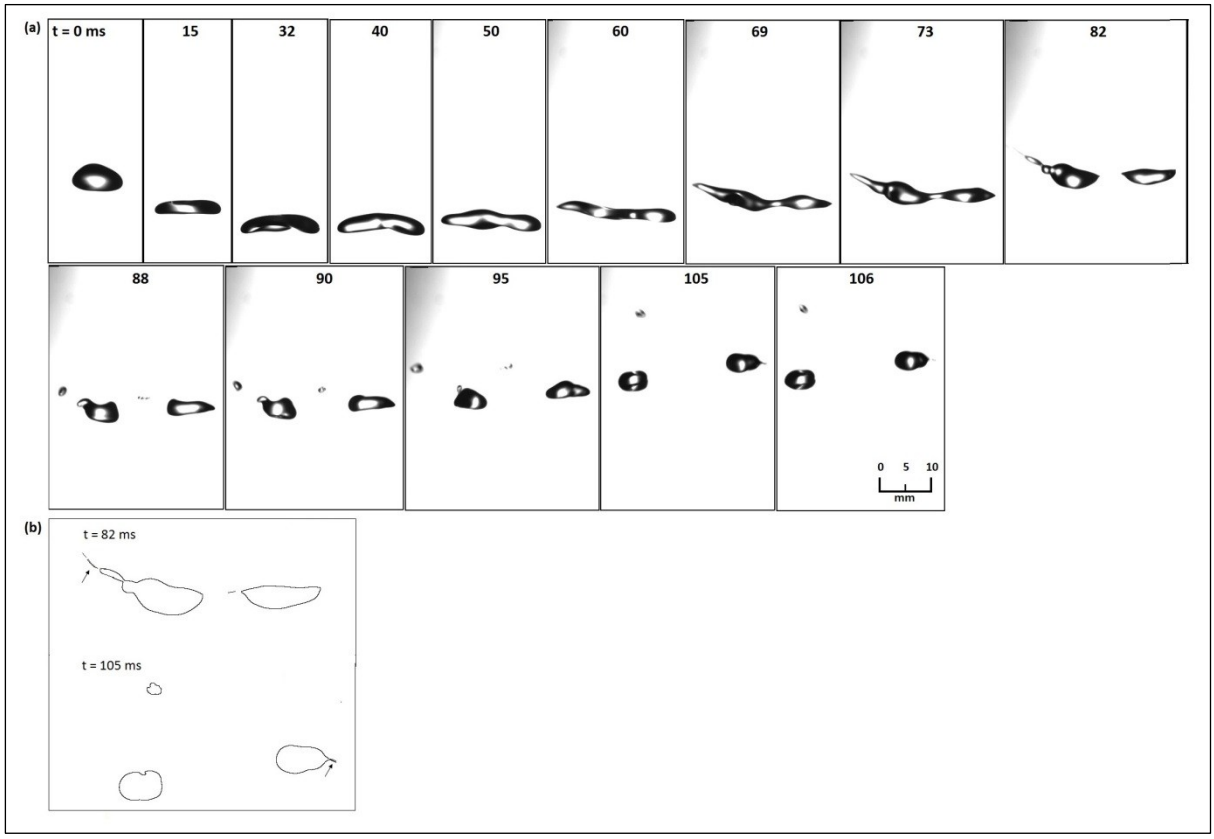

Figure 20 (a) *Photographs illustrating the occurrence of extreme elongation followed by the breakup of a drop of 7.0 mm diameter in the presence of the horizontal electric field of 500 kVm^{-1}. Time shown in each frame indicates the evolution of breakup in ms.* ***(b)*** *Schematic diagram of frames at t = 83 and 105 ms in Figure 4a showing a fine jet spray of droplets ejected indicated by an arrow from one sharp end at t = 83 ms of the drop and another jet spray at t =105 ms from the other end of the drop.*

6.6 Bag breakup in absence/presence of electric field

As defined in section 6.4, bag type of breakup occurs when the concavity of the drop develops rapidly into an expanding bag which ultimately bursts into multiple smaller droplets whilst the annular ring breaks up into a few larger droplets. Occasionally, a fine spray of droplets was observed from the annular ring in the process of development of bag portion [Blanchard, 1949,1950; Magarvey and Taylor, 1956, Villermaux and Bossa, 2009]. In our experiment we observed bag type of breakup in ~ 12 % of the drops in $E_H = 0$. However, it was never observed in $E_H = 500$ kVm^{-1} for the same drop sizes [Bhalwankar et al., 2017]. To verify the occurrence of bag breakup in the vertical electric field (E_V) we photographically captured ten events of drop breakup of 7.25 mm diameter in a relatively low electric field of $E_V = 300$ kVm^{-1}. Our observations prominently reveal bag type of breakup in ~ 40 % cases

with multiple smaller droplets from bag portion, few larger droplets and occasionally a fine spray of droplets from the annular ring as shown in Figure 21. The observations, though based on a statistically small number of breakup events, definitely indicate that the E_V may enhance the possibility of the bag breakup. The increasing probability of bag type of breakup in the vertical electric field of thunderclouds may introduce a large number of smaller droplets and modify the drop size distribution and thus affect the development of precipitation and electrification in thunderclouds.

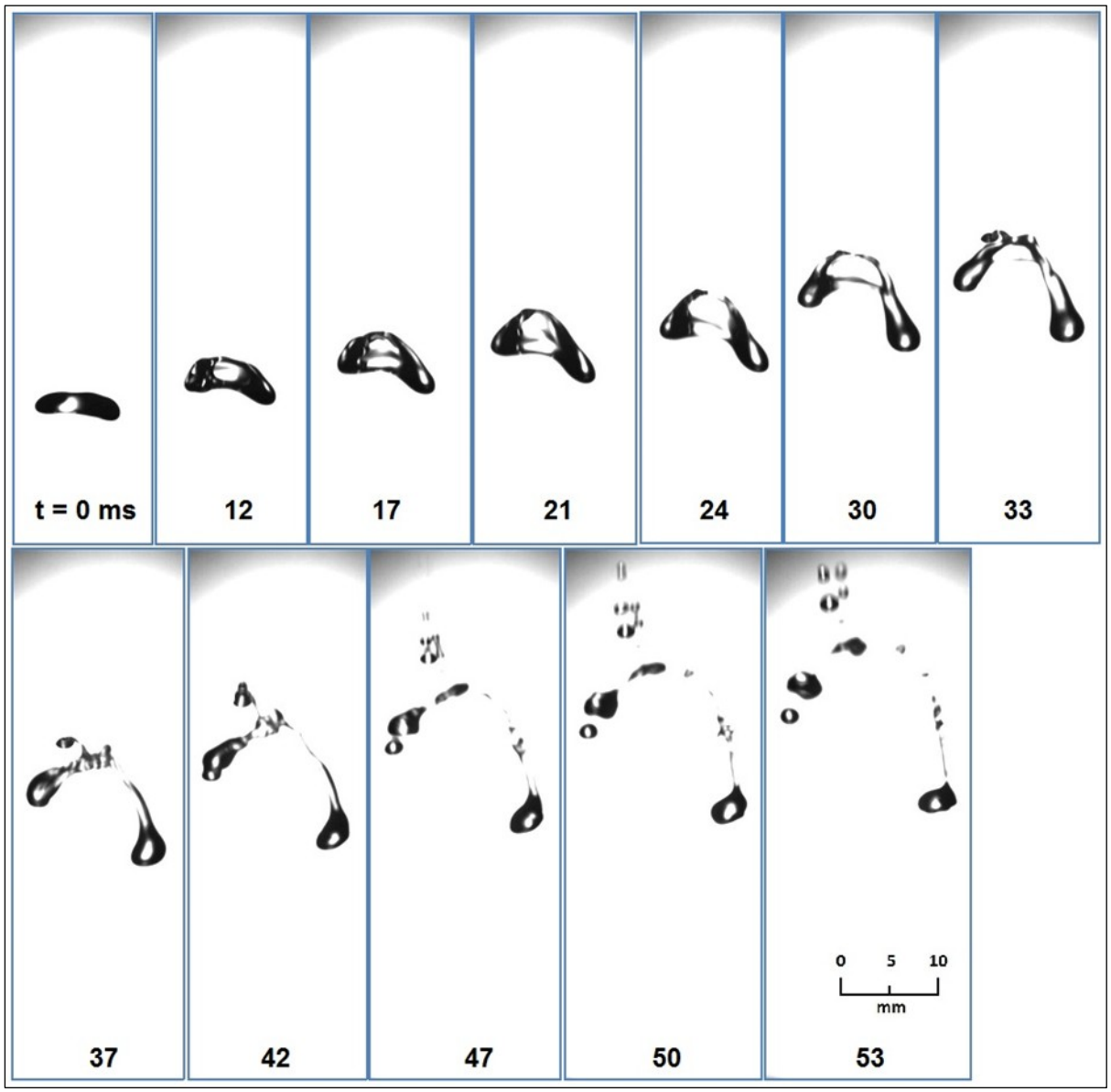

Figure 21. *The topological changes in a suspended drop of 7.0 mm diameter and its breakup in the presence of the vertical electric field of 300 kVm^{-1}. Time shown in each frame indicates the evolution of breakup in ms.*

Table 1. Number of drop breakup, and the ranges and the average values (given in bracket) of breakup time, oscillation frequency, time period of oscillation, elongation length, and mode of breakup of drops of different sizes in absence and presence of horizontal electric field

Diameter (mm)	Number of Breakups	Breakup Time (ms)	Oscillation Frequency (Hz)	Time period of Oscillation (ms)	Drop Elongation length (mm)	Mode of Breakup
$E_H = 0$ kVm^{-1}						
6.6	8	13-34 (27)	17-20 (18.6)	50 - 59 (54)	9.9-11.9 (10.5)	D = 5 F = 3 B = 0
7.0	10	14-41 (28)	15-19 (17.3)	53-67 (58)	10.6-14.8 (12.3)	D = 6 F = 3 B = 1
7.25	10	15-34 (29)	15-18 (16.9)	56-67 (59)	10.2-15.9 (12.9)	D = 5 F = 3 B = 2
$E_H = 500$ kVm^{-1}						
6.6	7	69-73 (70)	20-21 (20.8)	47-50 (48)	12.4-17.7 (14.98)	D = 0 F = 7 B = 0
7.0	11	57-93 (78)	17-19 (18)	53-59 (56)	14-19.05 (15.8) 29*	D = 0 F = 10 B = 0 EE = 1
7.25	12	66-105 (82)	16-17 (16.6)	59-63 (60)	17.8-20.7 (17.08) 42*	D = 0 F = 11 B = 0 EE = 1

D = Dumbbell mode; F = Filament mode; B = Bag mode; EE = Breakup with extreme elongation; * Length of extreme elongation in mm

Table 1 summarizes the results obtained in our experiment for the number and mode of drop break-up, ranges and average values (given in bracket) of breakup time, oscillation frequency, time period of oscillation and elongation length observed for different drop sizes in the absence or presence of electric field [Bhalwankar et al., 2017]. While the average frequency of the drop oscillations undergoes a small decrease, the average values of both breakup time and elongation length increase with the increase in drop size and in presence of the electric field. Although, these changes are small, these are observed consistently for all drop sizes in both absence and presence of the electric field. Small decrease in oscillation frequency with drop diameter has been earlier observed by Szakáll et al. [2010] and Bhalwankar et al. [2015].

6.7 Drop Breakup Charging

The phenomenon of drop breakup is known to produce charged and uncharged fragments [Lenard, 1921; Zeleny, 1933; Matthews and Mason, 1964]. When the drop breaks up in an electric field, the charges induced on the drop surface may modify the charges on the fragments. In our experiment, it was possible to determine the polarity of the charge on droplets after the drop breakup by tracking the drift of the filaments from the vertical in subsequent frames. Positively charged droplets had their vertical trajectory drifting towards negative electrode and negatively charged droplets towards the positive electrode.

Figure 22 (a and b) displays two typical events of the breakup of drops of 7.25 mm diameter in E_H = 500 kVm^{-1}[Bhalwankar et al., 2017]. At t = 87 ms in Figure 22a and at t = 89 ms in Figure 22b, drop breaks up forming two droplets – larger droplet having bulk of water and smaller droplet that includes the filament. Larger and smaller droplets carry opposite charges as seen from their movements away from each other and towards the electrodes of opposite polarity in subsequent frames. Larger (smaller) droplet is negatively (positively) charged in Figure 22a, the opposite is the case in Figure 22b. It shows that the polarity of charge on the two droplets after its breakup is determined by the induced charges on the parent drop by the prevailing electric field. Moreover, smaller droplets because of their lower terminal velocity move upward faster than the larger droplets. Figure 22 (a and b, respectively) demonstrates another interesting aspect of drop breakup. Soon after their breakup (frames at 95 and 97ms in Figure 22 a and b) the filament in smaller droplet quickly squeezes into smaller droplet. In doing so, it passes its momentum to the smaller droplet, causing it to eject a tiny droplet from the opposite side of the smaller droplet. Polarity of charge on these tiny droplets is also determined by the induced charges on the smaller droplet [Bhalwankar et al., 2017].

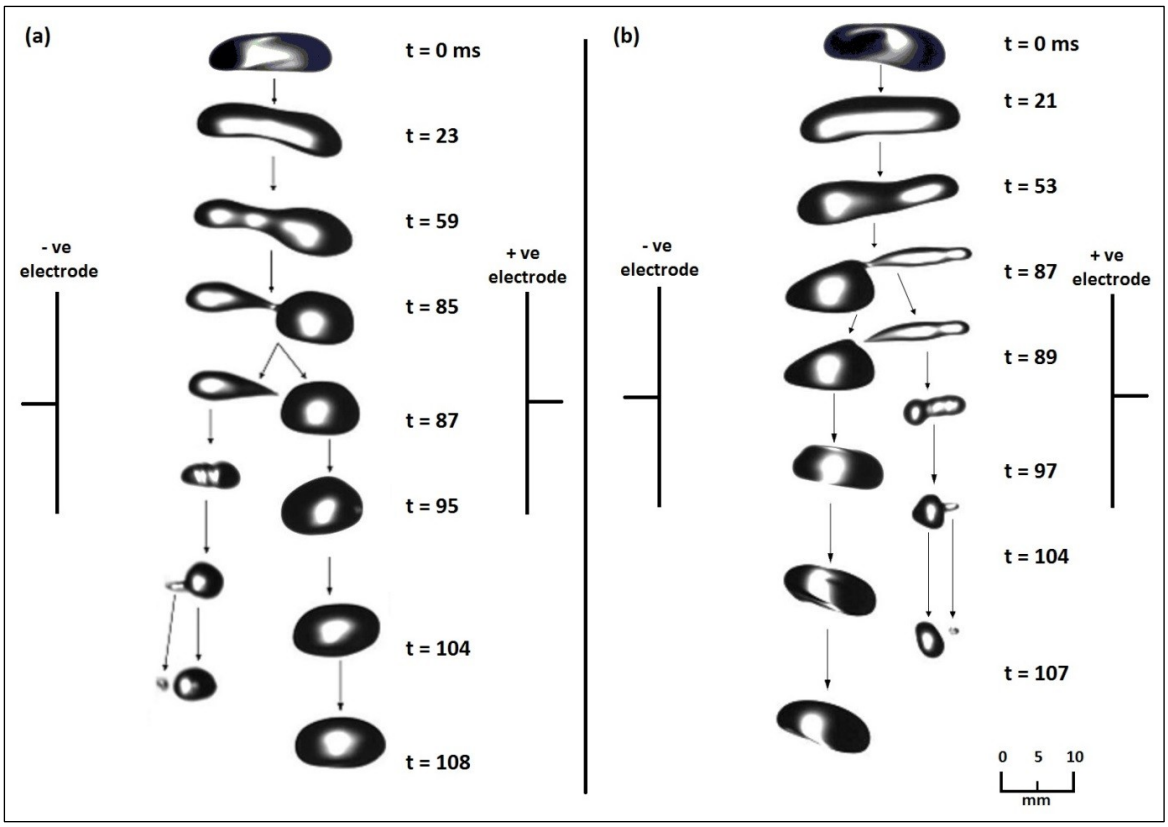

Figure 22. *Photographs of two typical events of breakup of water drops of 7.25 mm diameter and ejections of tiny droplets in the horizontal electric field of 500 kVm^{-1}.*

6.8 Distortion and breakup of polluted water drops in horizontal electric fields

Increasing industrialization and human activities in industrial area are continuously pumping the gaseous and aerosol pollution to the atmosphere. As a result, the clouds forming over industrial areas and big cities get highly polluted and incidences of acidic rain have often been reported over such areas [Huff, and Changnon, 1973; Westcott, 1995; Sanusi et al., 1996]. Shape and behavior of polluted raindrops in such clouds is likely to considerably change an account of the change in forces that determine the shape of the drop. In order to investigate this problem, we conducted some experiments, in which the water drops suspended in the tunnel, were formed from distilled water or from 100 ppm solutions of ammonium sulphate or potassium nitrate [Bhalwankar and Kamra, 2009]. Electrical conductivity of these solutions was measured with a conductivity meter. The conductivity values of distilled water and solution of ammonium sulphate and potassium nitrate are 1.10 149.4 and 110.6 μS cm-1, respectively. The values of surface tension, viscosity, and density of the polluted drops calculated from Tables given by Lange and Forker [1967] show an increasing trend with respect to distilled water.

Variation of axis ratio of a water drop formed from distilled water and sulphate/nitrate solutions, with horizontal electric field is shown in Figure 23.

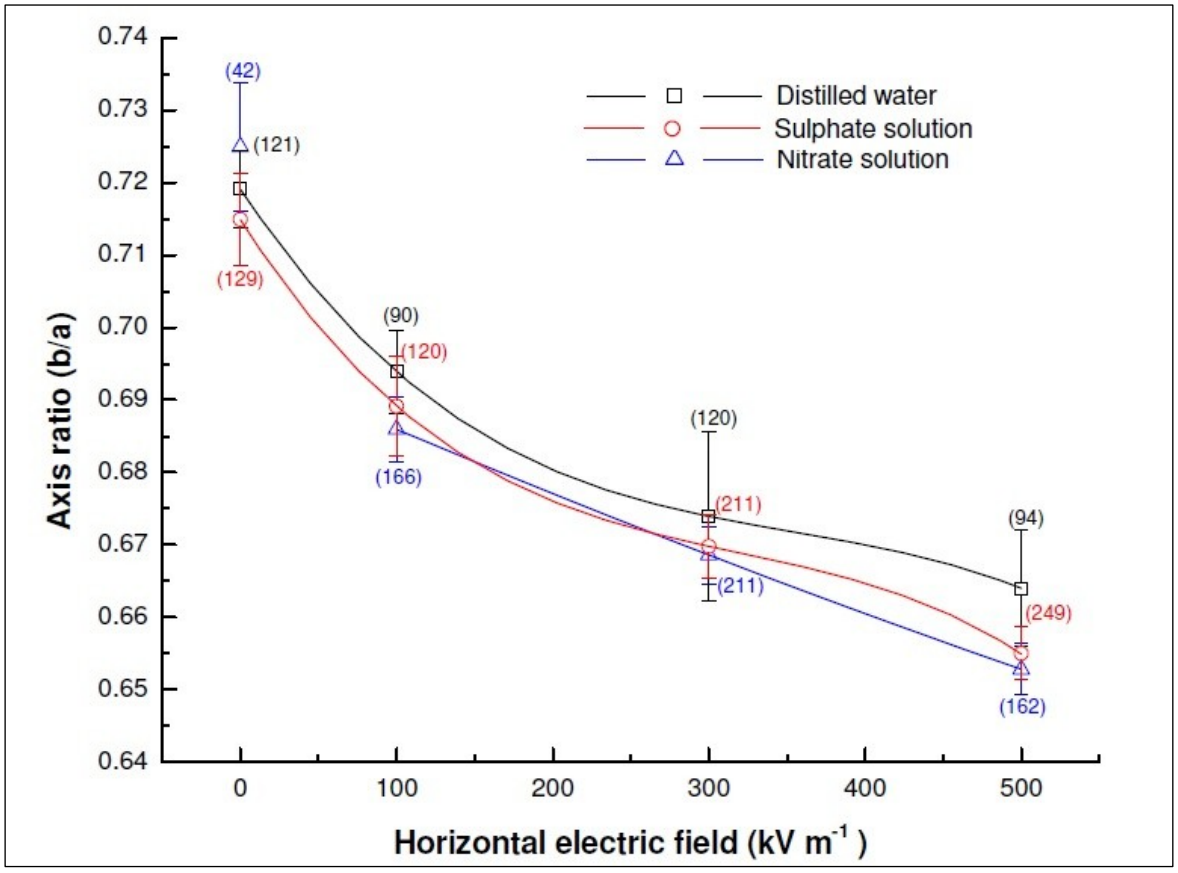

Figure 23. *Variation of axis-ratio (b/a) of a water drop of 4.05 mm diameter formed from distilled water and sulphate /nitrate solutions, with horizontal electric field. For calculating the average point in case of nitrate solution, only 42 images could be obtained because of some technical difficulties. Therefore, though plotted in figure, it is not considered for drawing the best-fit curve for nitrate solution.*

Results show that the oblateness of the drops increases when the drops are formed from the water polluted with sulphate/nitrate salts. The enhanced distortion of polluted drops with horizontal electric field is the combined effect of the enhanced induced charges on the surface of water drops and the attraction of cations and anions along the direction of electric field. On the other hand, the salt concentration in water increases the surface tension force, density and viscosity which try to keep the drop spherical and resist the fluid flow within the drop during its oscillation and reduce the amplitude of oscillations of the polluted drops. Thus, the enhanced deformation of the polluted drop and the electrical forces acting on its surface feedback each other during its oscillatory phase for drop breakup to occur more readily than that of uncharged drops [Bhalwankar et al., 2014].

7. Discussion

The series of simulation experiments performed in our wind tunnel provides a good set of observations in demonstrating the way in which the E_H manifests its effect in influencing the shape of a drop at various stages of its distortion, onset of corona discharge from its surface and leading it to its eventual breakup.

External vertical or horizontal electric fields elongate the drop along the direction of electric field. The horizontal electric field is more efficient in distorting the drop because the electric force acts to enhance the drop's distortion in the direction in which the drop is already distorted in no electric field. The action of E_H in distorting a drop is described below and explained systematically with the help of a schematic diagram in Figure 24. In the case of a spherical drop, the electric field at the surface of the drop is distorted to be 3-fold of the ambient electric field (Figure 24a). However, since the large drops are already distorted to oblate shape, the horizontal electric field is enhanced around the lower ring of the drop and tends to elongate the major axis of the oblate-shaped drop (Figure 24b). Consequently, water in the drop sinks down from its upper to lower portion to reduce the concavity of its upper half. Minor axis of drop therefore reduces and the drop tends to change from oblate shape to sheet shape (Figure 24c). The effect of the E_H is, therefore, not only to elongate drop's major axis but also to reduce its oblateness and ultimately to make it sheet-shaped. Such an action of E_H continues to suppress the formation of any blobs and suppress the concavity of the drop surface as the drop further elongates horizontally (Figure 24d). As the drop elongates further, the electric field at the extreme ends of the sheet-shaped drop gets intensified to the extent that this enhancement of the field further elongates the drop. Thus, the drop's distortion and electrical force acting on the drop, feedback each other in further elongation of the drop [Kamra et al., 1993]. Consequently, both ends of the drop develop sharp curvature (Figure 24e). Roughly, during the same period, the sharp curvature emits a jet spray of very small droplets. A fine jet spray occurs at this stage at the either end of the drop with a time difference. Finally, the sharp curvature of the drop's surface and the filament which develops in the middle of the drop breaks up and form small droplets (Figure 20b; drop at t = 90 ms in Figure 20a).

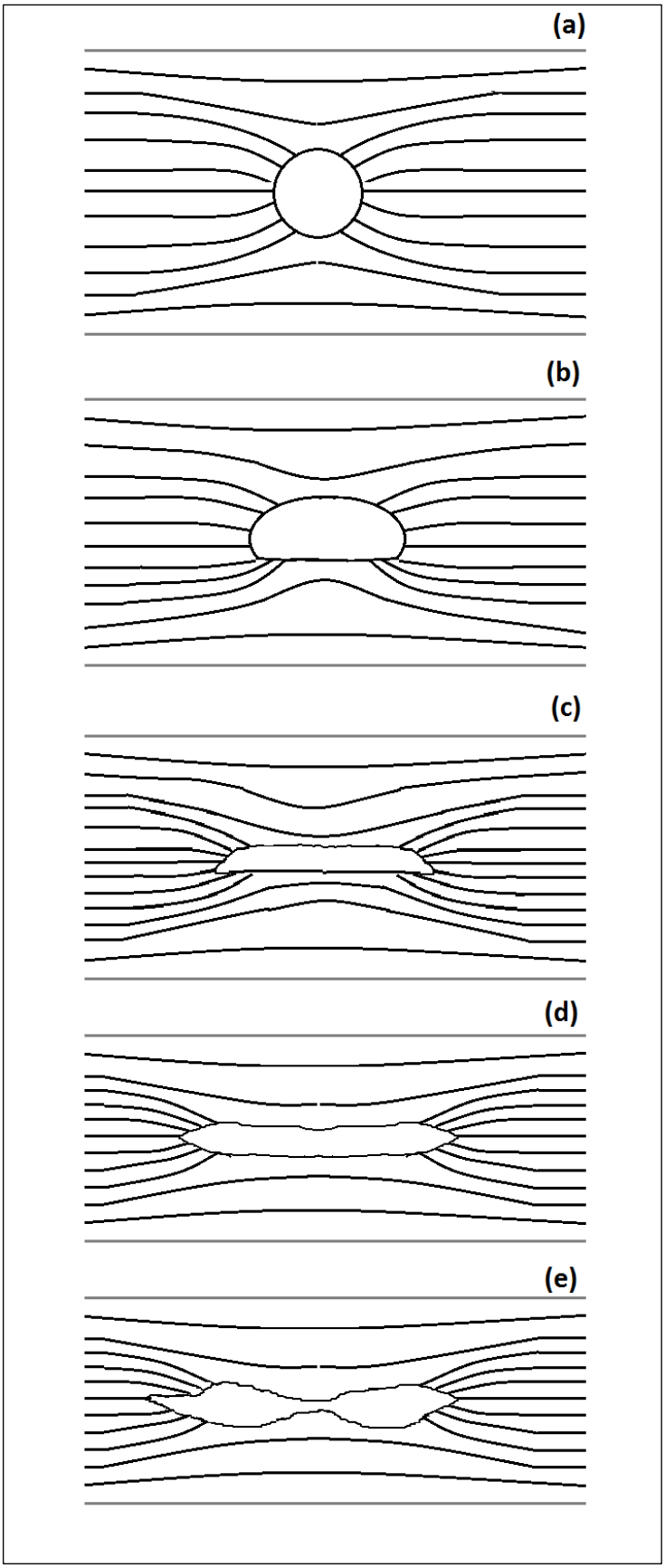

Figure 24. *Schematic diagram showing the deformation of the drop shape and the horizontal electric field configuration at various stages of the drop's deformation.*

A water drop suspended in wind tunnel also experiences oscillations and rotations around its vertical minor axis. So, the maximum amplitude of the horizontal axis of the drop is oriented in different directions during its oscillations. When the orientation of maximum amplitude of horizontal axis of the drop coincides with the direction of the horizontal electric field, elongation of the drop attains its maximum amplitude. In this position of the maximum elongation, the drop will be most unstable and will have maximum probability of breakup. Moreover, the edges of the drop are likely to be sharpest in this position and may develop corona if the local field on the surface is sufficiently enhanced.

The enhanced deformation observed in case of polluted drop suspended in horizontal electric field is likely to be a consequence of the increase in surface tension, viscosity and density [Bhalwnkar and Kamra , 2009]. Particularly, the dramatic increase in conductivity of polluted drops is likely to be a dominant factor for modifying the magnitude and polarity of charge in the particle collisions and in the initiation and propagation of lightning discharge in the clouds formed in polluted environments [Bhalwnkar and Kamra , 2013]. The fact that the electric charge, free or induced by an electric field, resides on drop's surface may be the key factor in this respect. Higher conductivity of polluted raindrops can influence the cloud electrification by (1) enhancing the charging of interacting drops through a non-inductive mechanism [Jayaratne et al., 1983], (2) changing the sign reversal temperature between the interacting drops [Williams, 2001], (3) impacting the graupel charge polarity with temperature through the change in cloud droplets spectrum caused by the pollutants [Avila et al., 1999)].

Enhanced distortion of polluted drops in horizontal electric field observed in the experiment of Bhalwankar and Kamra (2009) will lower down the critical value of ambient electric field for onset of corona emission from the drop surface. On the other hand, the decrease in amplitude of the drop oscillation observed will decrease the probability of occurrence of corona discharge at a given field. Further, the micro-discharges from polluted drops observed by Boussaton et al. (2005), can sustain a stable streamer propagation and thus enhances the probability of leader formation [Schroeder et al., 1999]. A propagating streamer is more easily initiated, the threshold for sustained discharge propagation is reduced, and branching is more developed if the water drops are polluted [Tardiveau and Marode 2003; Temnikov et al., 2003; Williams et al., 1985].

The relative roles of the electrical and other forces in breaking the drops are very well illustrated in the case of the extreme elongation in Figure 20 (a and b). Initially, the balance of all forces, mainly determines the oblate shape and the oblate-prolate oscillation

characteristics of the drop. However, once the drop gets excessively elongated, say after t = 40 ms in Figure 20a, the feedback process between the electrical forces and drop's distortion dominates the drop elongation. This feedback process, although elongates the drop to greater lengths, is slower than the former process. This explains the greater length of elongation and longer time period required for the breakup of drop in E_H as observed in our observations.

It is also significant to note that although bag type of breakup was observed in 12% of drops in $E_H = 0$, none of the drops exhibited bag type of breakup in $E_H = 500$ kVm^{-1} in our experiment. The observation strongly suggests that the development of any concavity on the upper surface (downstream side) and any depression at the lower surface (base/upstream side) of the drop is suppressed by the E_H simply because E_H tends to stretch the drop in the horizontal direction. Since the base depression is believed to be responsible for the hydrodynamic breakup [Pruppacher and Klett, 2010], its suppression would decrease the probability of such breakup as observed in our observations. Results imply that the drop size distribution is influenced by the magnitude and direction of electric field.

Various studies, outlined above, provide a strong evidence to suggest that the distortion and breakup of water drops can lead to large variability in the occurrence of lightning on the both, spatial and temporal scales in the thunderclouds developing over clean and polluted areas. The change in lightning may be more pronounced over the regions of big cities, forest fires, oil refineries etc. as observed by Westcott (1995), Murrey et al. (2000), Orville et al. (2001), Soriano and de Pablo (2002), Steiger et al. (2002) where the environment is highly polluted. However, an increase in lightning activity over larger scales of last one or two decades is also reported in South Asia (Ramesh Kumar and Kamra, 2012). It needs to be investigated whether such changes are taking place on global scale due to the global increase in the background concentration of the atmospheric aerosols in industrial era.

8. Significance of the results in thunderclouds

Although large-scale electric fields in thunderclouds are mostly vertical, the raindrops falling in a thundercloud pass through different regions where both the magnitude and direction of electric field differ. While the magnitude of electric field may be of the order of several hundreds of kilovolts per meter, their direction may have large inclination from the vertical [Winn and Moore, 1971; Stoltzenburg and Marshall, 1998]. Moreover, the electrical charge carried by raindrops in thunderclouds may approach Rayleigh's limit [Rust and Moore, 1974; Gaskell et al., 1978]. Drop charges may also vary with the direction of electric field in the induction type of charging mechanism [Kamra, 1977]. Electrical forces acting on raindrops in such intensely electrified environments of thunderstorms may be comparable to

the gravitational forces acting on them and may limit the charge separation process by the falling precipitation mechanisms [Kamra, 1970, 1975, 1979a; Kamra and Vonnegut, 1971; Gay et al. 1974]. Several models [e.g. Griffith and Latham, 1974; Scott and Levin, 1975; Mason, 1972; Moore, 1974; Palurch and Sartor, 1973] of thunderstorm charging have included the effect of such large electrical forces acting on drops. Such electrical forces may also create regions of accumulation of precipitation particles in thunderclouds [Kamra, 1982a] and modify the electrical conductivity of the air in thunderclouds [Kamra, 1979b] and even influence the initiation and intensity of downdrafts in a thundercloud [Kamra, 1982b; Bala and Kamra, 1991].

Results of our laboratory simulation experiments show that the electrical forces acting on a drop falling in presence of a horizontal electric field stretch the drop along its major axis and enhance its oblateness. On the contrary, the electrical forces in presence of vertical electric fields stretch the drop along its minor axis and tend to make it spherical in shape. So, in contrast to the tendency of the drop becoming more unstable with the increasing size in horizontal electric field, the vertical electric fields first tend to make it more stable. However, at very high values of vertical electric fields, the drop becomes prolate in shape and unstable. Above results imply that smaller drops may attain the critical value for breakup and are more likely to break in those regions of clouds where the prevailing electric field is horizontal rather than vertical. This implies that the size distribution of drops is expected to be wider and therefore the drop-growth is likely to be faster in those regions of cloud where vertical rather than horizontal electric fields prevail. Whether this difference in drop size-distribution can be used to locate the regions of cloud having different directions of electric field by remote sensing, needs to be investigated.

Breakup of a raindrop in the rain shaft region or below the melting band of thunderclouds is one of the important mechanisms affecting the drop size distributions. Our observations show that the E_H can influence not only the mode of drop breakup, but also drastically change the number, size and charge carried by the smaller droplets formed after the drop breakup. A significant observation made in our experiment is that the bag type of drop breakup which is prevalent in the absence or is enhanced in the vertical electric field is not observed in the presence of the horizontal electric field. Bag type of breakup is known to add a large number of very small droplets when the bag breaks up. On the other hand, the size and charge of the droplets produced after dumbbell type of breakup in the absence of an electric field and from the filaments or sharp curvature of the horizontally elongated drop's surface drastically differ from each other. Such changes in the mode of breakup can

significantly change the size and charge distributions of the drops in the regions of the horizontal electric field in thunderclouds. This is likely to change the drop growth and thus the development of rain by the collision-coalescence process [Testik et al., 2011].

Long exposure of the drop to the horizontal electric field in our experimental set-up facilitated the exceptional elongation of the drop along its major axis in E_H = 500 kVm^{-1} developing several sharp points and thin filaments on drop which can produce corona in the enhanced electric field around them [Richards and Dawson, 1971; Kamra et al., 1993; Coquillat et al., 2003]. Further, the tiny droplets emitted from the sharp curvature of the elongated drop's surface and the small droplets produced after drop breakup can be transported to a mixed-phase region in thunderclouds where they can participate in cloud electrification processes. Corona emitted from such water drops can trigger lightning discharges in thunderclouds [Griffiths, and Latham, 1972; Kamra et al., 1993; Coquillat et al., 2003]. Further, the change in the size distribution of cloud drops may modify the radar echo – precipitation relationships in regions of thunderclouds with different directions of electric field [Bhalwankar and Kamra, 2007].

The electric force acting on water drops influences their growth and evaporation, both within clouds and during their fall in the sub-cloud layer. Thus, it is essential to include the ventilating effect of drop's motion on their rate of evaporation. Our experimental results show that the rate of evaporation of charged drops is slower than that of uncharged drops of the same size. Such highly charged drops develop a pronounced oblate distortion caused by the charge density enhancement at their waist [Kamra et al., 1991]. This change in shape of charged drops alters the airflow around them and consequently results in a decrease in their ventilation coefficient. The above results also show that some raindrops falling from an electrified thunderstorm to the sub-cloud layer may evaporate at a lesser rate than those falling from a weakly electrified cloud.

Most of the drops inside thunderstorms are likely to be little influenced by the above results because the value of relative humidity inside thunderstorms is mostly close to 100% and only a small fraction of drops may carry a charge in excess of 10^{-10} C. However, these results are applicable to the drops which fall close to the edges of rainshaft and undergo considerable evaporation and thus approach their charge limit. The evaporation of drops in the dry air below thunderstorms is quite important in some regions, for example, in the southwestern United States, where sometimes all the water drops falling below cloud bases evaporate before reaching the ground. This kind of rain is called `virga'. Zrink *et al* (1984) suggested that the change in drop shape due to surface charge might be detected in the

differential reflectivity of radar signal from electrically active thunderstorms, particularly just before the lightning.

Most of the studies dealing with the role of aerosols in modifying the cloud electrification give strong evidence that cities inadvertently affect the electrical and microphysical characteristics of the clouds that develop in such polluted environments and these modified characteristics can interact in such a way so as to enhance the rainfall, cloud electrification and lighting activity [Murray et al., 2000; Rosenfeld and Woodley, 2001; Steiger et al., 2002; Westcott, 1995]. Several studies show that surface active chemical compounds may significantly reduce the rate of evaporation and growth by condensation of drops [Pruppacher and Klett 2010 and references therein]. Our results imply that the microphysical effects caused by such pollutants include a reduction of the surface tension, an increase in drop deformation, a dampening of drop oscillation and an enhancement of drop breakup [Ryan, 1976; Bhalwankar and Kamra, 2009]. The break-up of water drops which is observed to occur more readily in polluted clouds will narrow down their size distribution [Bhalwankar and Kamra, 2014].

9. Conclusions

The present results obtained for the behavior of raindrops suspended in the vertical, horizontal or no electric field configurations in our experiments have the unique advantage of being obtained under similar conditions in the same experimental set-up. Moreover, the values of the electric field and drop diameter considered in our experiment, although in the higher range, do exist in the bases and in small pockets of the intensely electrified regions of thunderclouds. Further, the drops are suspended at their terminal velocities and spend sufficient time in electric field to undergo large number of oscillations about their equilibrium shapes while they are exposed to the electric field. Hence, the relative results obtained in our laboratory simulation experiments can be applied to raindrops in clouds with a higher degree of confidence.

Results from our long series of experiments well demonstrate that electrification of cloud strongly interacts with its microphysical properties. Electrical forces acting on the drop surface either by the drop being charged or being located in electric field, influence its terminal velocity, shape, deformation, evaporation and breakup characteristics. Both, the magnitude and direction of electric field play a crucial role in this interaction. Our experiments demonstrate that horizontal electric fields are much more effective in influencing these drop characteristics. During the breakup process, the drop introduces a large number of small charged /uncharged droplets in the cloud. This will change the size and charge

distributions of the drops and consequently the development of the precipitation in clouds. As a consequence of these electrical effects, thunderclouds may develop some regions of in-homogeneities in their microphysical properties. Also, such interactions may result in some variabilities in the rainfall-radar echo relationships in radar meteorology.

Observation of corona from water drops suspended in horizontal electric fields in our experiment is at much lower values of electric fields than those reported in earlier studies where drops were placed in a vertical electric field. This result is likely to solve the long-standing problem of the triggering of lightning in thunderclouds at much lower electrical field than the dielectric breakdown value of the air. Further, enhanced distortion of polluted drops and increased probability of their breakup in horizontal electric field observed in our experiment may explain the triggering of lightning at lower values of electric field in the polluted than unpolluted clouds. This may help explain the higher lightning flash rates observed over big cities, industrial areas and regions of forest fire in many studies.

10. Suggestions for future work

1. Development of new experimental techniques and theoretical models is needed in which behavior of both charged as well as uncharged drops can be studied in presence of electric field in different directions.
2. Various results presented in this report strongly emphasize the need to develop parameterization schemes to include the interactions of clouds electrification with their microphysics in theoretical models for the development of precipitation in clouds. There is urgent need for such efforts to improve our skills in now-casting.
3. Effects need to be made to better understand the role of corona from the drop surface in horizontal electric fields in initiating and propagation of lightning streamers in thunderclouds.
4. Better understanding of the interaction between cloud electrification and microphysics is needed for improving the radar echo-rainfall relationships for an accurate assessment of rainfall from radar echoes with higher resolution in space and time.

Acknowledgements

IITM was fully supported initially by Department of Science and Technology (DST) of the Ministry of Science & Technology upto 2006 and now by Ministry of Earth Sciences, Govt. of India. Authors acknowledge all the Directors, IITM, for the encouragement in carrying out this work during this period. AKK acknowledges the support under the INSA (Indian National Science Academy) Honorary Scientist programme.We are also thankful to our colleague, A.B. Sathe, retired from the Institute, for his invaluable efforts in construction, installation of the wind tunnel and some initial experiments.

References

Abbas, M.A. and J. Latham, (1969), The disintegration and electrification of charged water drops falling in an electric field, Q. J. R. Meteorol. Soc., 95, 63-76,.

Ackerman, A.S., O.B. Toon, J.P.,Taylor, D.W. Johnson, P.V. Hobbs and R.J. Ferek, (2000), Effects of aerosols on cloud albedo: evaluation of Twomey's parameterization of cloud susceptibility using measurements of ship tracks, J. Atmos. Sci., 57, 2684–2695, doi.10.1175/1520-0469(2000)057o2684: EOAOCA42.0.CO;2..

Andsager, K., K.V. Beard and N.F. Laird, (1999), Laboratory measurements of axis ratios for large raindrops, J. Atmos. Sci., 56 (15), 2673-2683.

Ausman, E.L. and M. Brook, (1967), Distortion and disintegration of water drops in strong electric fields, J. Geophys. Res., 72, 6131–6135.

Avila, E.E., R.G. Pereyra, G. G. A. Varela and G. M. Caranti, (1999), The effect of the cloud droplet spectrum on electrical charge transfer during individual ice–ice collisions, Q. J. R. Meteorol. Soc. 125, 1669–1679.

Bala, S.S. and A.K. Kamra, (1991), Change in precipitation drag due to thunderstorm electrification, Atmos, Res., 26, 377-387, 1991.

Beard, K.V., (1984). Raindrop oscillations: evaluation of a potential flow model with gravity, J. Atmos. Sci., 41, 1765– 1774.

Beard, K.V. and C. Chuang, (1987), A new model for the equilibrium shape of raindrops, J. Atmos. Sci. 44, 1509–1524.

Beard K.V., H.T. Ochs and R.J. Kubesh, (1989b), Natural oscillations of small raindrops, Nature, 342, 408-410.

Beard, K.V., D.B. Johnson, and D. Baumgardner, (1986), Aircraft observations of large raindrops in warm, shallow, convective clouds, Geophys. Res. Lett., 13, 991-994.

Beard, K.V., R.J. Kubesh, H. T. Ochs III, (1991), Laboratory measurements of small raindrop distortion, Part I: Axis ratio and fall behavior. J. Atmos. Sci. 48, 698 – 710.

Beard, K.V. and R.J. Kubesh, (1991), Laboratory measurements of small raindrop distortion Part II: Oscillation frequencies and modes. J. Atmos. Sci., 48, 2245–2264.

Beard, K.V. and H.R. Pruppacher, (1969), A determination of the terminal velocity and drag of small water drops by means of a wind tunnel, J. Atmos. Sci. 25, 1066 -1072.

Beard, K.V. and H.R. Pruppacher, (1971), A wind tunnel investigation of the rate of evaporation of small water drops falling at terminal velocity in air, J. Atmos. Sci. **28** 1455-1464

Beard, K.V. and A. Tokay, (1991), A field study of small raindrop oscillations. Geophys. Res. Lett. 18 (12), 2257–2260.

Bhalwankar R.V., A.B. Sathe and A.K. Kamra, (2004), The evaporation of the charged and uncharged water drops suspended in a wind tunnel, Proc. Indian Acad. Sci. (Earth Planet. Sci.), 113,129-138.

Bhalwankar, R. V. and A. K. Kamra, (2007), A wind tunnel investigation of the deformation of water drops in the vertical and horizontal electric fields, J. Geophys. Res., 112, D10215, doi:10.1029/2006JD007863.

Bhalwankar, R.V. and A.K. Kamra, (2009), A wind tunnel investigation of the distortion of polluted water drops in the horizontal electric fields, J. Geophys. Res., VOL. 114, D10205, doi:10.1029/2008JD011102.

Bhalwankar, R.V. and A.K. Kamra, (2013), Role of drop distortion in enhancing the lightning activity in clouds formed over cities, J. Atmos. Sol. Terr. Phys. 94, http://dx.doi.org/10.1016/j.jastp.2012.12.018, 65-70.

Bhalwankar, R.V., S. Subramanian and A.K. Kamra, (2014), Laboratory simulation of spontaneous breakup of polluted water drops in the horizontal electric field, J. Atmos. Sol. Terr. Phys., http://dx.doi.org/10.1016/j.jastp.2014.07.013.

Bhalwankar, R., C.G. Deshpande, and A.K. Kamra, (2015), Shape and oscillations of the waterdrops freely suspended in a horizontal electric field: A wind tunnel study, J. of Atmos. Sol.Terr. Phys. 133, 169–177, http://dx.doi.org/10.1016/j.jastp.2015.09.004.

Bhalwankar, R., C.G. Deshpande, and A. K. Kamra, (2017), Breakup modes of the drops suspended in a vertical wind tunnel in presence of the horizontal electric field, J. Geophys. Res. Atmos., 122, 1838–1849, doi:10.1002/2016JD025805.

Blanchard, D.C., (1949), Experiments with water drops and the interactions between them at terminal velocity in air, Occas. Rep. 17, Proj. Cirrus, Gen. Electr. Res. Lab., Schenectady, N.Y., 29.

Blanchard, D.C., (1950), The behavior of water drops at terminal velocity in air, Eos. Trans. AGU, 31, 836-842.

Blanchard, D.C., (1953), Raindrop size-distribution in Hawaiian Rains, J. Meteorol., 10, 457-473, 1953.

Boussaton, M.P., S. Coquillat, S. Chauzy and J.F. Georgis, (2005), Influence of water conductivity on micro-discharges from raindrops in strong electric fields, Atmos. Res. 76, 330– 345, doi:10.1016/j.atmosres.2004.

Brazier-Smith, P.R., (1971), The stability of water drops oscillating with finite amplitude in an electric field. J. Fluid Mech. 50, 417– 430.

Bringi, V.N. and V. Chandrasekar, (2004), Polarimetric Doppler Weather Radar: Principles and Applications, Chembridge University press.

Chandrasekar,V., W.A. Cooper, and V.N. Bringi, (1988), Axis ratios and oscillations of raindrops, J. Atmos. Sci., 45, 1323-1333.

Chuang, C. and K.V. Beard, (1990), A numerical model for the equilibrium shape of electrified raindrops, J. Atmos. Sci., 47, 1374–1389.

Coquillat, S., B. Combal and S. Chauzy, (2003), Corona emission from raindrops in strong electric fields as a possible discharge initiation: Comparison between horizontal and vertical field configurations, J. Geophys. Res., 108(D7), 4205, doi:10.1029/2002JD002714, ACL 1-16.

Coquillat, S. and S. Chauzy, (1993), Behavior of precipitating water drops under the influence of electrical and aerodynamical forces, J. Geophys. Res. 98,10,319–10,324, doi:10.1029/93JD00389.

Coquillat, S. and S. Chauzy, (1994), Computed conditions of corona emission from raindrops, J. Geophys. Res., 99, 16,897-16,905.

Coquillat, S., B. Combal and S. Chauzy, (2003), Corona emission from raindrops in strong electric fields as a possible discharge initiation: Comparison between horizontal and vertical field configurations, J. Geophys. Res., 108(D7), 4205, doi:10.1029/2002JD002714, ACL 1-16.

Dawson, G.A. and R.A., Warrender, (1973), The terminal velocity of raindrops under vertical electric stress, J. Geophys. Res., 78, 3619-3620.

Emersic, C. and P.J. Connolly, (2011), The breakup of levitating water drops observed with high speed camera, Atmos. Chem. and Phys., 11(19), doi: 10.5194/acp-11-11739.

Feingold, G., S. Tzivion and Z. Levin, (1988), The evolution of raindrop spectra. Part I, Stochastic collection and breakup, J. Atmos. Sci., 45, 3387-3399.

Fitzerald, D.R. and H.R. Byers, (1962), Aircraft electrostatic measurement instrumentation and observations of cloud electrification, Rept., contract AF 19(604)2189, University of Chicago.

Gaskell, W., A.J. Illingworth, J. Latham and C.B. Moore, (1978), Airborne studies of electric fields and the charge and size of precipitation elements in thunderstorms; Q. J. R. Meteorol. Soc., 104, 447-460.

Gay, M.J., R.F. Griffiths, J. Latham, and C.P.R. Saunders, (1974), The terminal velocity of charged raindrops and cloud droplets falling in strong electric fields, Q.J.R. Meteor. Soc., 100, 682-687.

Green, A.W., (1975), An approximation for the shapes of large raindrops, J. Appl. Meteor. 14 (8), 1578–1583.

Griffiths, R.F. and J. Latham, (1972), The emission of corona from falling drops, J. Meteorol. Soc. Jpn., 50, 416-422.

Griffiths, R.F. and J. Latham, (1974), Field generation and dissipation currents in thunderclouds as a result of movement of charged hydrometeors, J. Atmos. Sci., 32, 958-964.

Hegg, D.A., P.V. Hobbs and L.F. Raschke, (1994), Measurements of the scavenging of sulfate and nitrate in clouds, Atmos. Environ., 18, 1939-1946.

Huff, F.A. and S.A. Changnon, (1973), Precipitation modification by major urban areas, *Bull* Amer Meteorol Soc, 54,1220-1232.

Jayaratne, E.R., C.P.R. Saunders and J. Hallett, (1983), Laboratory studies of the charging of soft-hail during ice crystal interactions, Q. J. Roy. Meteorol. Soc., 109, 609–630.

Johnson, D.B. and K.V. Beard, (1984), Oscillation energies of colliding raindrops, J. Atmos. Sci., 41, 1235-1241.

Jones, D.M.A., (1959), The shape of raindrops, Journal of Meteorology 16, 504-510.

Jones, B.K. and J.R., Saylor, (2009), Axis ratios of water drops levitated in a vertical wind tunnel, J. Atmos. Ocean Technol. 26(11), 2413-2419.

Jones, B.K., J.R. Saylor and F.Y. Testik, (2010), Raindrop Morphodynamics, Chapter 2, Rainfall: State of the Science, Geophysical Monograph Series 191.

Kamra, A.K., (1970), Effect of electric field on charge separation by the falling precipitation mechanism in thunderclouds, J. Atmos. Sci., 27, 1182-1185.

Kamra, A.K. and B. Vonnegut, (1971), A laboratory investigation of the effect of particle collisions on the generation of electric fields in thunderstorms, J. Atmos. Sci., 28, 640.

Kamra, A.K., (1975), The role of electrical forces in charge separation by the falling precipitation mechanism in thunderclouds, J. Atmos. Sci., 32(1), 143-157.

Kamra, A.K., (1977), Effect of the inclination of the electric field on the inductive charging mechanism in thunderclouds, J. Atmos. Sci., 34, 681-683.

Kamra, A.K., (1979a), Effect of electrical forces on charge separation caused by the combined effect of the precipitative and convective mechanisms in thunderclouds, J. Geophys. Res., 84, 5039-5045.

Kamra, A.K., (1979b), Contributions of cloud and precipitation particles to the electrical conductivity and the relaxation time of the air in thunderstorms, J. Geophys. Res.,84, 5034, 1979.

Kamra, A.K., (1982a), Changes in concentrations of cloud and precipitation particles in the highly electrified regions of thundercloud, J. Geophys. Res., 87, 11,215-11,221.

Kamra, A.K., (1982b), Possible effect of the cloud electrification on the downdraft in thunderstorms, Geophys. Res. Lett., 9, 235-238.

Kamra, A.K. and D.V. Ahire, , (1985), A simple technique for simultaneous suspension of multiple drops in a small vertical wind tunnel, J.Atmos. and Oceanic Tech., 408-411.

Kamra, A.K., A.B. Sathe and D.V. Ahire, (1986), A vertical wind tunnel for drop studies Mausam, 37, 2, 219-222.

Kamra, A.K. and D.V. Ahire, (1989), Wind-tunnel studies of the shape of charged and uncharged water drops in the absence or presence of an electric field, Atmos. Res. 23 (2), 117–134.

Kamra, A.K., R.V. Bhalwankar and A.B. Sathe, (1991), Spontaneous breakup of charged and uncharged water drops freely suspended in a wind tunnel. J. Geophys. Res. 96, 17,159–17,168, doi:10.1029/91JD01475.

Kamra, A.K., R.V. Bhalwankar and A.B. Sathe, (1993), The onset of disintegration and corona in water drops falling at terminal velocity in horizontal electric fields, J. Geophys. Res., 98, 12,901 – 12,912, doi:10.1029/93JD00625.

Komabayasi, M., T. Gonda and K. Isone, (1964), Lifetime of water drops before breaking and size distribution of fragment droplets, J. Meteorol. Soc. Jpn. 42(II), 330-340.

Kinzer G.D. and R. Gunn,(1951), The evaporation, temperature and thermal relaxation time of freely falling water drops, J. Meteorol*.,* **8,** 71-83.

Krehbiel, P.R., R.J. Thomas, W. Rison, T. Hamlin, J. Harlin and M. Davis, (2000), GPS-based mapping system reveals lightning inside storms, Eos Trans., 81, 21-25, AGU, Washington, D.C.

Kubesh, R.J. and K.V., Beard, (1993), Laboratory measurements of spontaneous oscillations for moderate-size raindrops, J. Atmos. Sci. 50 (8), 1089–1098.

Kumar, P.R. and A.K. Kamra, (2012), Variability of lightning activity in South/Southeast Asia during 1997–98 and 2002–03 El Nino/La Nina events. Atmospheric Research, 118, 84-110.

Lamb, H., (1945), Hydrodynamics. Dover Publications, New York.

Lange, N.A. and G.M. Forker, , (1967), Handbook of Chemistry, McGraw Hill, New York.

Langmuir, I., (1948), The production of rain by a chain reaction in cumulus clouds at temperature above freezing, J. Meteorol., 5, 175-192.

Lenard, P., (1904), Über Regen. Meteorl. Z. 21, 248-262 (for English translation see: Quart. J. Roy. Meteor. Soc., 31, 62-73).

Lenard, P. (1921), Zur Wasserfalltheorie der Gewitter, Ann phy., 65, 629-639.

Low, T.B. and R. List, (1982a), Collision, coalescence and breakup of raindrops, Part I, Experimentally established coalescence efficiencies and fragment size distribution in breakup, J. Atmos. Sci., 39, 1591-1606.

Low, T.B. and R. List (1982b), Collision, coalescence and breakup of raindrops, Part II, parameterization of fragment size distribution, J. Atmos. Sci., 39, 1607-1618.

Macky, W.A., (1931), Some investigations on the deformation and breaking of water drops in strong electric fields, Proc. R. Soc. London, Ser.A,133, 565-587.

Magarvey, H.R. and W.B. Taylor, (1956), Free fall breakup of large drops, J. Appl. Phys., 27, 1129-1135.

Marshall, T.C. and W.D. Rust, (1991), Electric field soundings through thunderstorms, J. Geophy. Res., 96, D12, 22,297-22,304 DOI: 10.1029/91JD02486.

Marshall, T.C. and W.P. Winn, (1982) Measurements of charged precipitation in a New Mexico Thunderstorm: Lower positive charge centres; *J. Geophys. Res.,* **87,** 7141-7157.

Mason, B.J., (1952), production of rain and drizzle by coalescence in stratiform clouds, Q.J.R.Meteor. Soc 78, 377-386.

Mason, B.J., (1972), The physics of thunderstorm. Proc. Roy. Meteor. Soc., A327, 433-466.

Matthews, J.B. and B.J. Mason (1964), Electrification produced by the rupture of large water drops in an electric field, Q. J. R. Meteorol. Soc., 90, 275-286.

McFarquhar, G.M. (2004a), A new representation of collision-induced breakup of raindrops and its implication for the shape of raindrop size distribution, J. Atmos. Sci., 61, 777-794.

McTaggart–Cowan, J.D. and R. List (1975), Collision and breakup of water drops at terminal velocity, J. Atmos. Sci., 32, 1401-1411.

Moore, C.B., (1974), An assessment of thundercloud electrification mechanisms, in Elelctrical Processes in Atmospheres, edited by R. Reiter and H. Dolezalek, Dietrich Stienkopff, Darmstadt, Germany.

Murray, N.D., R.E. Orville and G. R. Huffines, (2000), Effect of pollution from Central American fires on cloud-to-ground lightning in May 1998, Geophys. Res. Lett. 27, 2249–2252.

Nolan, J.J., (1926), The breaking of water drops by electric fields, Proc. R. Ir. Acad., Sect., 8, 3--7, 28-39.

Orville, R.R., G. Huffines, J.N. Gammon, R. Zhang, B. Ely, S. Steiger, S. Phillips, S. Allen and W. Read, (2001), Enhancement of cloud-to-ground lightning over Houston, Texas. Geophys. Res. Lett. 28 (13), 2597–2600.

Palunch, I.R. and J. D. Sartor, (1973), Thunderstorm electrification by the inductive charging mechanism: I. Particle charges and electric fields, J. Atmos. Sci., 30, 1166-1173.

Pruppacher, H.R. and K.V. Beard, (1970), A wind tunnel investigation of the internal circulation and shape of water drops falling at terminal velocity in air. Quart. J. Roy. Meteor. Soc. 96, 247–256.

Pruppacher, H.R. and J.D. Klett, (2010), Microphysics of Clouds and Precipitation, Spriger, Dordrecht, Netherlands.

Pruppacher, H.R. and R.L. Piter, (1971), A semi-empirical determination of shape of cloud and raindrops. J. Atmos. Sci. 28, 86–94.

Pruppacher, H.R. and R. Rasmussen, (1979), A wind tunnel investigation of the rate of evaporation of large water drops falling at terminal velocity in air, J. Atmos. Sci., 36, 1255-1260.

Rayleigh, J.W.S., (1879), On the capillary phenomena of jets. Proc. Roy. Soc. London. 29, 71–97.

Rasmussen, R., C. Walcek, H.R. Pruppacher, S.K. Mitra, J. Lew, V. Levizzani, P.K. Wang and U. Barth, (1985), A wind tunnel investigation of the effect of an external, vertical electric field on the shape of electrically uncharged rain drops. J. Atmos. Sci. 42, 1647–1652.

Reisin T.G., Yan Yin, Z. Levin and S. Tzivion, (1998), Development of giant drops and high-reflectivity cores in Hawaiian clouds: numerical simulations using a kinematic model with detailed microphysics, Atmos. Res., 45, 275-297.

Richards, C.N. and G.A. Dawson, (1971), The hydro-dynamic instability of water drops falling at terminal velocity in vertical electric fields, J. Geophys. Res., 75, 3445-3455.

Rosenfeld, D. and W.L. Woodley, (2001), Pollution and Clouds, Physics World. Institute of Physics Publishing LTD, Dirac House, Temple Back, Bristol BS1 6BE, UK, February 2001, 33–37.

Rust, W.D. and C.B. Moore, (1974), Electrical conditions near the bases of thunderclouds over New Mexico, Q. J. R. Meteorol. Soc., 100, 450-468.

Ryan, R.T., (1976), The behavior of large, low-surface-tension water drops falling at terminal velocity in air, J. Appl. Meteorol., 15, 157–165.

Sanusi, A., H. Wortham, M. Millet and P. Mirabel, (1996), Chemical composition of rainwater in eastern France, Atmos. Environ. 30, 59-71.

Savic, P., (1953), Circulation and distortion of liquid drops falling through a viscous medium, Natl. Res. Council, Canada, Rep. NRC-MT-22, 50 pp.

Saylor, J.R. and B.K. Jones, (2005), The existence of vortices in the wakes of simulated raindrops, Physics of Fluids, 17(3). 031716.

Schroeder, V., M.B. Baker and J. Latham, (1999), A model study of corona emission from hydrometeors, Q. J. R. Met. Soc., 125, 1681–1693, doi:10.1002/qj.49712555710.

Scott, W.D. and Z. Levin (1975), A stochastic electrical model of an infinite cloud; charge generation and precipitation development, J. Atmos. Sci., 32, 1814-1828.

Soriano, L.R. and F. de Pablo, (2002), Effect of small urban areas in central Spain on the enhancement of cloud-to-ground lightning activity, Atmospheric Environment, 36, 2809–2816.

Siliga T.A. and V.N. Bringi, (1976), Potential use of radar differential reflectivity measurements at orthogonal polarizations for measuring precipitation, J. Appl. Meteor. 15, 69–76.

Steiger, S.M., R.E. Orville and G. Huffines, (2002), Cloud-to-ground lightning characteristics over Houston, Texas: 1989–2000, J. Geophys. Res. 107 (D11) doi:10.1029/2001JD001142.

Stolzenburg, M. and T. C. Marshall, (1998), Charged precipitation and electric field in two thunderstorms, J. Geophys. Res., D103, 19777-19790.

Szakáll, M., K. Diehl, S.K. Mitra and S. Borrmann, (2009), A wind tunnel study on the shape, oscillation and internal circulation of large raindrops with sizes between 2.5 and 7.5 mm, J. Atmos. Sci. 66, 755 – 765, doi:10.1175/2008JAS2777.1.

Szakáll, M., S.K. Mitra, K. Diehl and S. Borrmann, (2010), Shapes and oscillations of falling raindrops - a review. Atmos. Res. 97, 416–425.

Szakáll, M., S. Kessler, K. Diehl, S.K. Mitra and S. Borrmann, (2014), A wind tunnel study of the effects of collision processes on the shape and oscillation for moderate-size raindrops, Atmos. Res. 142, 67-78.Taylor, G. (1964), The disintegration of water drops in an electric field, Proc. R. Soc. London, Ser. A, 280, 383-397.

Taylor, G., (1964), The disintegration of water drops in an electric field. Proc. R. Soc. London, Ser. A, 280, 383-397.

Testik, F.Y. and A.P. Barros, (2007), Toward elucidating the microstructure of warm rainfall: A survey, Review of Geophysics, 45, 2, DOI: 10.1029/2005RG000182.

Testik, F. Y., (2009), Outcome regimes of binary raindrop collisions, Atmos. Res., 94, 389–399.

Testik, F.Y., A.P. Barros and L. F. Bliven, (2011), Toward a physical characterization of raindrop collision outcome regimes, J. Atmos. Sci., 68, 1097-1113, http://dx.doi.org/10.1175/2010JAS3706.1

Tardiveau, P. and E. Marode, (2003), Point-to-plane discharge dynamics in the presence of dielectric droplets. J. Appl. Phy., 36, 1204–1211, doi:10.1088/0022-3727/36/10/309.

Temnikov, A.G., I.P. Vereshchagin, A.V. Orlov and M.V Sokolova, (2003), Investigation of the main stage of a discharge between an artificially charged water aerosol cloud and a grounded electrode. in Proceedings of the 12th International Conference on Atmospheric Electricity, Int. Comm. on Atmos. Electr., Versailles, France, 549– 552.

Thurai, M. and V.N. Bringi, (2005), Drop axis ratios from 2d video disdrometer, J. Atmos. Oceanic Technol., 22(7), 966-978.

Thurai, M., M. Szakáll, V.N. Bringi, K.V. Beard, S.K. Mitra and S. Borrmann, (2009), Drop shapes and axis ratio distributions: comparison between 2d video disdrometer and wind-tunnel measurements. J. Atmos. Oceanic Technol. 26 (7), 1427–1432.

Tokay A. and K.V. Beard, (1996), A field study of raindrop oscillation, Part I, Observation of size spectra and evaluation of oscillation causes, J. Appl. Meteorol., 35, 1671-1687.

Tokay, A., Chamberlain, R., Schoenhuber, M., (2000), Laboratory and field measurements of raindrops oscillations. Phys. Chem. Earth. (B) 25,867-25,870.

Villermaux E. and B., Bosa, (2009), Single-drop fragmentation determines size distribution of raindrops, Nature Physics 5, DOI:10.1038/NPHYS1340, 697-702.

Villermaux, E. and B. Bossa, (2010), Size distribution of raindrops, Nature Physics, 6, 232.

Westcott, N.E., (1995), Summer time cloud-to-ground lightning activity around major Midwestern urban areas. J. Appl. Meteorol. 34, 1633-1642.

Williams, E.R., (2001), The Electrification of Severe Storms Meteorol Monograph 28(50), 527–561.

Williams, E.R., C.M. Cooke and K.A. Wright, (1985), Electrical discharge propagation in and around space charge clouds. J. Geophys. Res.90, 6059–6070, doi:10.1029/JD090iD04p06059.

Winn, W.P. and C.B. Moore, (1971), Electric fields Measurements in thunderclouds using instrumental rockets, J. Geophys. Res., 76, 5003-5017.

Winn, W.P., G.W. Schwede and C.B. Moore, (1974), Measurements of electric fields in thunderclouds, J. Geophys. Res., 79, 1761– 1767.

Zeleny, J., (1933), Variation with temperature of the electrification produced in air by the disruption of water drops and its bearing on the prevalence of lightning, Phys. Phys. Rev., 44, p. 837.

Zrink, D.S., R.J. Doviak and P.R. Mahapatra, (1984), The effect of charge and electric field on the shape of rain drops, Radio Science, 19, 75-80.